NASA CONTRACTOR REPORT

NASA CR-1589

STUDY OF THE APPLICATION OF A PHOTOIONIZATION MASS SPECTROMETER TO ANALYSIS OF CONTAMINANT GASES

by Peter Warneck, J. N. Driscoll, and C. Matthews

Prepared by
GCA CORPORATION
Bedford, Mass.
for Langley Research Center

NATIONAL AERONAUTICS AND SPACE ADMINISTRATION • WASHINGTON, D. C. • MAY 1970

NASA CR-1589

add e - T; Application ... gases.

STUDY OF THE APPLICATION OF A PHOTOIONIZATION MASS SPECTROMETER TO ANALYSIS OF CONTAMINANT GASES

By Peter Warneck, J. N. Driscoll, and C. Matthews

May 70

add e;
Issued by Originator as Report No. GCA-TR-69-10-N

Prepared under Contract No. NAS 8-mist 1-7794
m.e. GCA CORPORATION
Bedford, Mass.

for Langley Research Center

NATIONAL AERONAUTICS AND SPACE ADMINISTRATION

FOREWORD

This study was conducted by GCA Corp., Bedford, Massachusetts during the period of June 1966 through November 1969 under Contract NAS 1-7794.

For on-line monitoring of spacecraft cabin atmospheres it is often desirable to measure gases with nearly identical masses, i.e., carbon monoxide and nitrogen (mass = 28), and so forth. In general, it would be necessary to employ either a multiplicity of instruments, each designed to monitor a specific gas, or a sophisticated, high resolution mass spectrometer. The photoionization source spectrometer, because of its ability to selectively ionize different gases, is being investigated as a possible means of monitoring with a mass spectrometer of moderate resolution, and therefore greater simplicity. This approach has the further advantage that during at least part of a revolution of the spacecraft, ultra-violet radiation from the sun can be utilized, thus reducing demands upon the on-board power supply. Additional application of the approach is possible in such areas as metabolic studies based on breath analysis and monitoring of atmospheric constituents.

The program was sponsored by the Flight Instrumentation Division of the Langley Research Center and was conducted under the auspicies of the Biotechnology and Human Research Division of the Office of Advanced Research and Technology, NASA Headquarters.

Wesley C. Easley
Contract Technical Monitor

Walton L. Jones, Director
Biotechnology and Human
Research Division

TABLE OF CONTENTS

Section	Title	Page
	SUMMARY	1
I	INTRODUCTION	2
II	INSTRUMENTATION AND PROCEDURES	5
	A. General	5
	B. Light Sources	8
	C. Sample Inlet System	11
	D. Sample Preparation	16
	E. Operational Procedures	18
III	RESULTS	23
	A. General	23
	B. Mass Spectra	23
	C. Sensitivities	35
	D. Problems with NO_2	42
	E. Detection Limits	46
	F. Efficiency of Instrumentation	47
	G. Mixtures	51
IV	CONCLUSIONS	60
	A. Application to Trace Gas Analysis	60
	B. Application to the Analysis of Spacecraft Cabin Atmospheres	61
	REFERENCES	65

STUDY OF THE APPLICATION OF A PHOTOIONIZATION MASS SPECTROMETER TO ANALYSIS OF CONTAMINANT GASES

By Peter Warneck, J. N. Driscoll, and C. Matthews

SUMMARY

Thirty-two gases and vapors were investigated with the photoionization mass spectrometer described previously. Fragmentation patterns were determined at four ionizing wavelengths: 803, 950, 1048, and 1216Å, respectively, making use of strong line sources. The possibility of discriminating between isomeric substances by varying the wavelengths was found to exist for the butenes, and butylalcohols, but not for the xylenes. In addition to fragmentation patterns, the mass spectrometric sensitivities and detection limits were determined to evaluate the potential of the photoionization mass spectrometer technique for trace gas analysis. It is shown that with presently available light sources average detection limits are about 10 ppm, in agreement with previous results. An assessment is made to show that the detection limits can be improved. Finally, the feasibility of utilizing photoionization mass spectrometry for the analysis of space cabin atmospheres, using solar ionizing radiation, is demonstrated.

I. INTRODUCTION

The long-term physiological and other effects of closed cabin atmosphere contaminants has been of considerable concern in conjunction with the planning of such programs as long-range space exploration, submarine laboratories, etc. Taken together with the problems arising from industrial and urban pollution, they have created a need for the detection, characterization, and quantitative determination of atmospheric trace constituents. The associated gas analytical requirements have led to the development of new and/or improved instrumentation. One way followed by GCA during recent years was to investigate the feasibility of photoionization mass spectrometry for the outlined task. The development of a mass spectrometer employing a photoionization source, its evaluation and further improvement have been described in several previous reports (Ref. 1-3). The unique features of gas analysis by photoionization mass spectrometry have also been discussed previously (Ref. 4-6), and may be briefly summarized as follows:

(1) Photoionization when compared to electron impact ionization eliminates the need of a heated filament so that delicate samples do not suffer pyrolysis at the filament; thermal decomposition in the heated ionization box is precluded as well.

(2) The absence of a filament also minimizes outgassing and memory effects.

(3) Fragmentation in the mass spectra can be greatly curtailed by an appropriate choice of ionizing energy. Although this possibility exists also with electron impact sources that provide the necessary energy resolution, the resulting ion intensities are unsuitable here because the ionization cross sections for electron impact near threshold are low and they rise only slowly with electron energy. The cross sections for photoionization, by contrast, resemble a step function at threshold so that high values are attained rapidly with increasing energy.

(4) The use of a uv monochromator provides a convenient narrow band energy selector. An appropriate choice of ionizing energy will, in principle, enable the selective ionization of some components in a complex gas mixture, whereas other components with higher ionization energies are not affected. This procedure can reduce the overlap and interference of individual contributions to the overall mass spectrum.

While these features have been demonstrated by previous work in this laboratory, the applications were limited to a few interesting cases, and it remained to investigate the capabilities of the photoionization mass spectrometer on a broader scale. In particular, it was of interest to investigate mass spectra for a variety of gases and vapors as a function of ionizing wavelength. From the variation of the fragmentation patterns

with the wavelength, the optimum wave length range can then be selected for analytical problems. Specifically, it was of interest to determine if the variation of ionizing wavelength would permit the discrimination between isomeric structures. This type of information was to be supplemented with data on mass spectrometric sensitivities, as well as detection limits to provide an indication of the value of the photoionization mass spectrometer technique in the field of trace gas analysis.

The present report contains data of this nature for some thirty gases and vapors. The investigated substances are listed in Table 1. The additional information provided in this table gives for each substance the ionization energy, the corresponding threshold wavelength, the vapor pressure at room temperature, and the maximum permissible percentage of the substance in a carrier gas below the condensation point. Each of the listed compounds was investigated with respect to its fragmentation pattern, sensitivity and detection limit. In addition, five mixtures containing at least three substances were studied.

In Section II of this report the experimental equipment and procedures are described. The results are given in Section III. Finally, in Section IV an assessment is made concerning the application of photoionization mass spectrometry to the analysis of trace contaminants in the laboratory and, by a special instrument using solar ionizing radiation, to the analysis of spacecraft cabin atmospheres.

TABLE 1

LIST OF COMPOUNDS INVESTIGATED, THEIR IONIZATION POTENTIALS, THRESHOLD WAVELENGTHS, ROOM TEMPERATURE VAPOR PRESSURES, AND THE CORRESPONDING UPPER LIMIT CONCENTRATION IN A CARRIER GAS AT ATMOSPHERIC PRESSURE

COMPOUND	IONIZATION POTENTIAL (eV)	PARENT ION m/e	IONIZATION THRESHOLD WAVELENGTH (Å)	VAPOR PRESSURE AT 23°C (torr)	MAXIMUM AMOUNT OF SAMPLE IN FLASK (%)
Acetone	9.69	58	1279	215	31.7
Acetaldehyde	10.21	44	1214	> 760	100.0
Allyl Alcohol	9.69	58	1279	22	3.1
Ammonia	10.15	17	1221	> 760	100.0
Benzene	9.245	78	1341	86	11.3
Butene-1	9.58	56	1294	> 760	100.0
cis-Butene-2	9.13	56	1358	> 760	100.0
trans-Butene-2	9.13	56	1358	> 760	100.0
n-Butyl Alcohol	9.95	74	1246	6.2	0.816
iso-Butyl Alcohol	9.96	74	1252	11.0	1.44
sec-Butyl Alcohol	9.85	74	1259	15	1.97
tert-Butyl Alcohol	10.00	74	1244	35	4.61
Carbon Disulfide	10.08	76	1230	330	43.5
1,4-Dioxane	9.13	88	1358	37	4.87
Ethyl Acetate	10.11	88	1226	87	11.3
Ethylene Dichloride	11.12	98	1114	76	10.0
Formaldehyde	10.87	30	1140	> 760	100.0
Freon 11	11.77	136	1053	750	98.8
Hydrogen Chloride	12.74	36	973	> 760	100.0
Hydrogen Sulfide	10.46	34	1185	> 760	100.0
Methane	12.98	16	955	> 760	100.0
Methyl Alcohol	10.85	32	1142	113	14.9
Methylene Chloride	11.35	84	1092	390	51.4
Nitric Oxide	9.25	30	1340	> 760	100.0
Nitrogen Dioxide	9.78	46	1267	> 760	100.0
Phenol	8.50	94	1459	0.26	0.034
Propionaldehyde	9.98	58	1242	--- n o d a t a ---	
Sulfur Dioxide	12.34	64	1004	> 760	100.0
Toluene	8.82	92	1405	23	3.03
Vinyl Chloride	9.995	62	1239	> 760	100.0
m-Xylene	8.56	106	1444	7.2	0.94
o-Xylene	8.56	106	1444	5.9	0.77
p-Xylene	8.44	106	1462	7.8	1.02

II. INSTRUMENTATION AND PROCEDURES

A. General

The photoionization mass spectrometer employed in the present study has been described in detail in previous reports (Ref. 1-3). Briefly, the arrangement is as follows: light in the extreme uv spectral region is generated in a discharge source, dispersed by means of a Seya vacuum monochromator, and passed through the ionization chamber of a mass spectrometer. The light intensity is monitored with a sodium salicylate coated photomultiplier. Ions formed in the ionization chamber by photoionization of the sample gas are extracted, accelerated and focused onto the entrance aperture of a magnetic analyzer which serves to separate the various groups of ions according to their mass to charge ratio. The ion current emerging from the exit orifice of the analyzer is detected and converted to an amplified electron current by an electron multiplier. The signal is further amplified with an electrometer. Differential pumping is employed to achieve the required low pressures in the light source, the monochromator, the ionization chamber, the ion accelerating region, and the magnetic analyzer. This is accomplished by three diffusion pumps — one each for the monochromator, the accelerating region and the magnetic analyzer — backed by a mechanical pump. A second mechanical pump is used to maintain a sufficient pressure differential between the light source section and the monochromator. Auxiliary equipment includes power supplies, electronic controls, and pressure gauges. A complete list of the auxiliary equipment now available with the instrument is given in Table 2.

Previously, the monochromator had been equipped with a 1200 lines/mm gold-coated grating having a blaze angle for maximum efficiency at 1500Å. However, tests had shown that a similar grating, but coated with platinum and blazed for 750Å, provides a superior efficiency for the present application. Accordingly, the gold-coated grating was supplemented by one coated with platinum, and having a blaze wavelength of 750Å. The latter grating was used throughout the present work.

Another addition made recently and worth noting is a precise current monitor for the magnet coils of the mass analyzer. For a given accelerating voltage, the mass to charge ratio transmitted by the analyzer is determined by the size of the magnetic field, which in turn is proportional to the magnetic coil current on a wide current range. Although the magnet power supply is equipped with a current meter, it was found that its scale and precision was insufficient for an unequivocal identification of ionic mass, particularly at the upper end of the current range, where the mass spectrum crowds together as a result of the square relationship between transmitted ion mass and magnet current. The new ampere meter has a 6-inch scale of one hundred divisions and provides an accuracy of 1 percent.

TABLE 2

LIST OF AUXILIARY EQUIPMENT FOR
PHOTOIONIZATION MASS SPECTROMETER

ITEM	RANGE	USE
(1) High Voltage Power Supply and Regulator	0-5 kV	Light Source
(2) High Voltage Power Supply	0-2 kV	Ion Acceleration
(3) High Voltage Power	0-6 kV	Electron Multiplier
(4) DC Power Supply	0-10 amps	Magnet
(5) Programmer	--	Magnet Current
(6) Ammeter, 7 inch face	0-10 amps	Magnet Current
(7) Electrometer	10^{-5} - 10^{-13} amps	Electron Multiplier read-out
(8) High Voltage Power Supply	0-2 kV	Photo-Multiplier
(9) Micro-microammeter	10^{-2} - 10^{-10} amps	Photo-Multiplier read-out

TABLE 2 (Cont.)

ITEM	RANGE	USE
(10) Vacuum Gauge Control	0-100 microns	Ion Source
(11) Vacuum Gauge Control	0-2000 microns	Light source
(12a) Ionization Gauge Control and Tube	10^{-4}-10^{-8} torr	Analyze
(12b) Thermocouple Gauges	0-1000 microns	I Pump, Gas Filter

B. Light Sources

The light source employed previously features a repetitively pulsed spark discharge in a ceramic capillary. When operated with argon at pressures in the 30 to 80 micron pressure regime, the light source emits a spectrum rich in lines in the wavelength range 400 to 1000Å. It has been pointed out previously (Ref. 3, 6), that some of the radiation at shorter wavelengths penetrates the monochromator and reaches the ion chamber even when the monochromator grating is set to transmit the first order spectrum in the 800 to 1000Å wavelength region. The admixture of radiation of shorter wavelengths to the first order spectrum is due to the weaker second order in the spectrum and to scattered light. To eliminate these undesirable components, a gas filter has been incorporated in the entrance arm of the grating monochromator. Argon is a particularly suitable filtering gas, as its absorption features resemble a step function. Full transmission occurs at wavelengths greater than 790Å, whereas light of shorter wavelengths is effectively attenuated. This effect can be enhanced if the argon spark light source is operated at pressures higher than indicated above. A spectrum of the emission under these conditions is given in Figure 1.

Although the argon spark light source appears to provide the most intense and suitable light source for the wavelength region below 1000Å, it is not very useful at longer wavelengths. Since a great many gases and vapors ionize at wavelengths greater than 1000Å with little ion fragmentation, it was desirable to have a second light source available for the latter spectral region. Accordingly, the spark light source was supplemented by a GCA dc cold-cathode discharge light source. When operated with hydrogen the dc source supplies the familiar many line spectrum of hydrogen in the 900 to 1300Å wavelength region. There is also a considerable emission at much longer wavelengths, but few gases and vapors can be ionized at wavelengths much greater than 1300Å. This type of light source will also provide an intense emission of the resonance lines of the rare gases: argon, neon, and helium, when these gases are employed instead of hydrogen. A detailed description of the dc light source follows below.

A common design for a cold-cathode discharge tube is to use a water-cooled quartz or Pyrex capillary sealed into a hollow cathode and anode by O-rings. However, the cold cathode discharge tube described here differs from the more conventional type in that it uses a water-cooled cathode and allows the quartz capillary to run hot rather than cooling the capillary with a water jacket. The main advantage of this feature is that there is no danger of water entering the vacuum system should the capillary break.

Figure 2 shows a cross section of the light source and Figure 3 shows a breakdown of the individual components. Basically, the light source consists of a 4-inch quartz disc with a quartz capillary of 4-mm bore sealed into the disc through its center and normal to its surface.

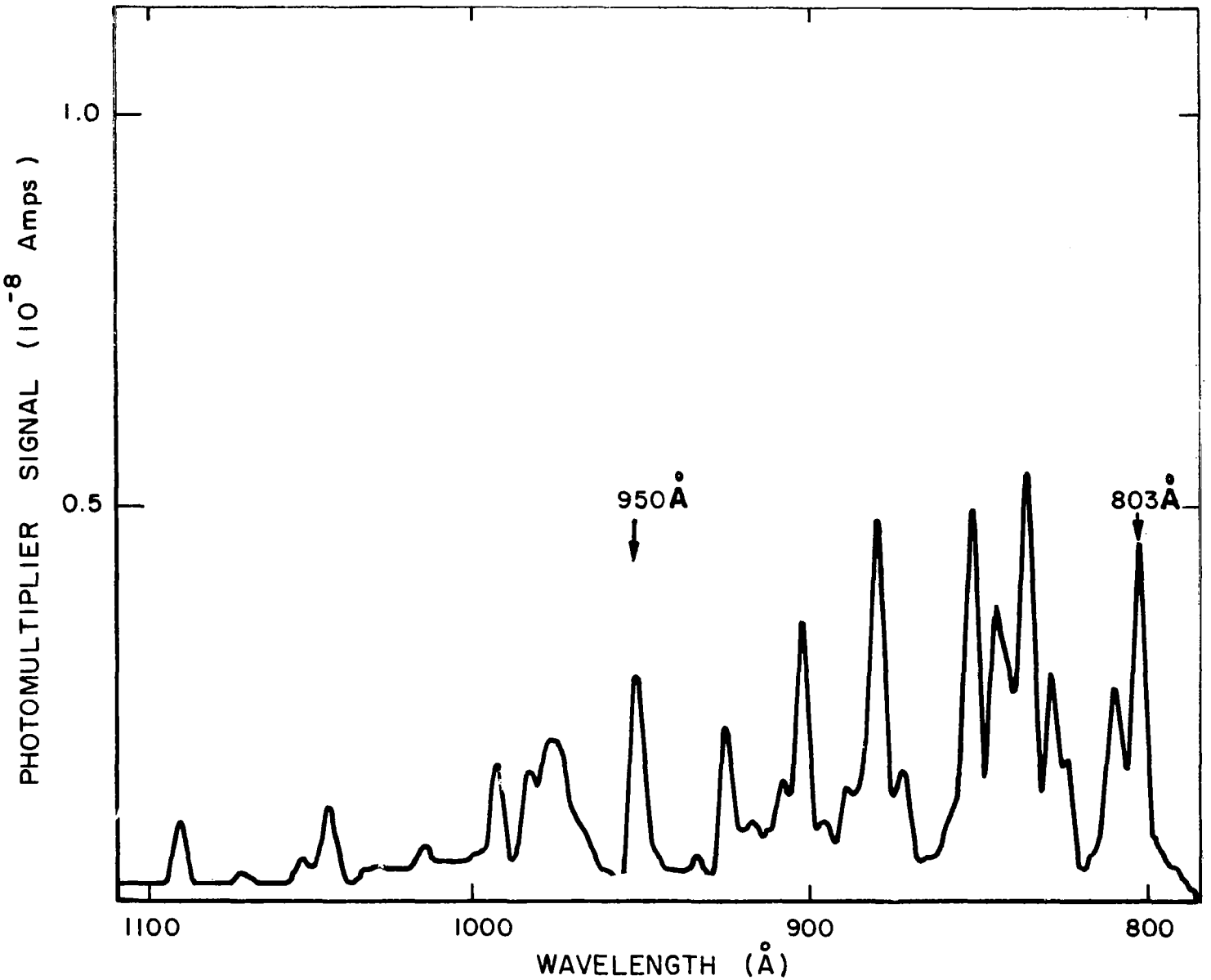

Figure 1. Argon spark source spectrum.

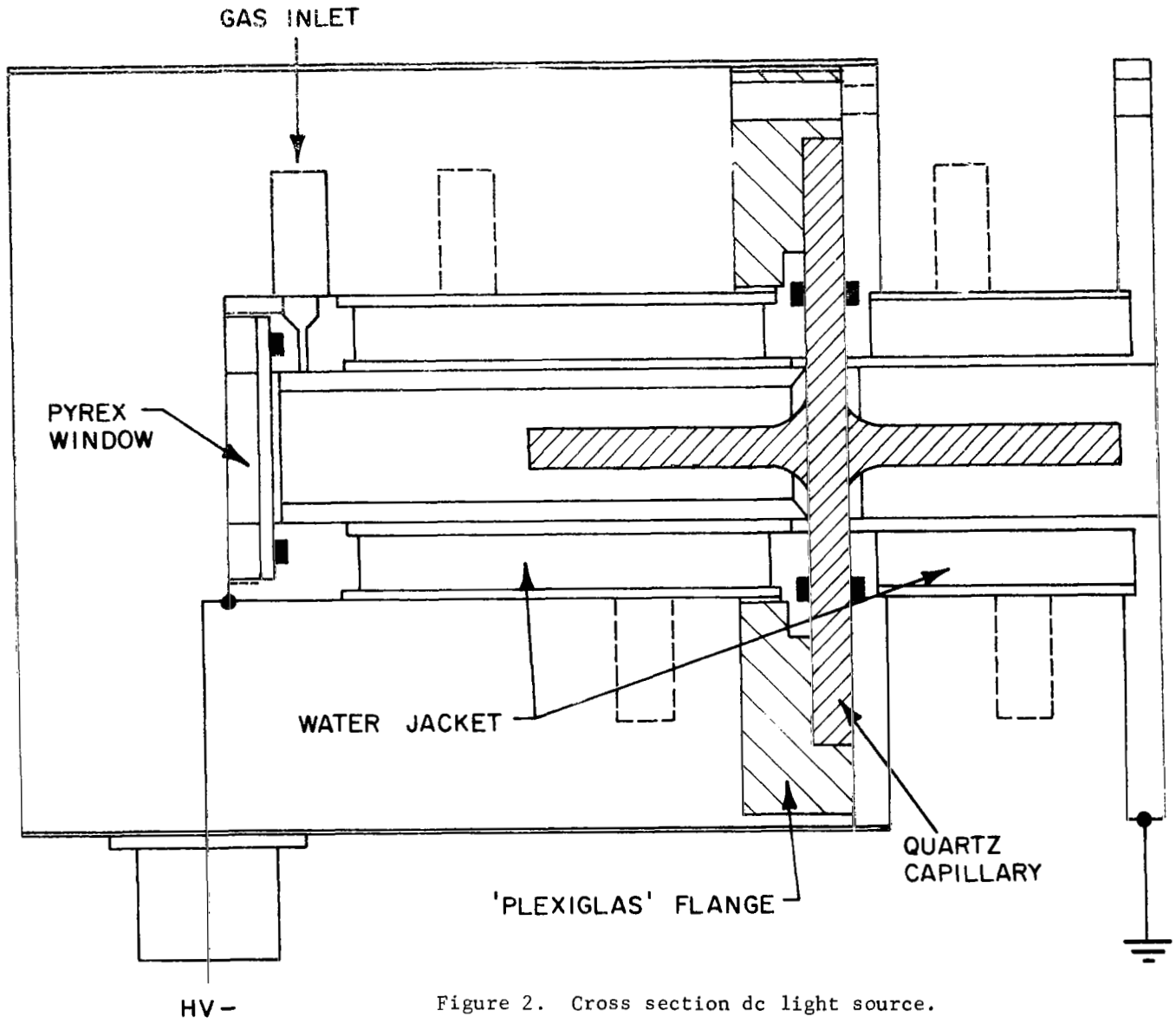

Figure 2. Cross section dc light source.

The quartz disc is ground flat to seat the O-rings on the cathode and the anode, and acts as an insulator as well as a vacuum seal. The cathode — the left-hand cylinder in Figure 3 — is constructed of two concentric cylinders sealed to allow water to flow between them. A hollow aluminum cylinder is seen protruding from the cathode. It actually acts as the cathode electrode, allowing easy replacement if necessary. The aluminum insert has a few very fine holes to allow the discharge gas to leak into the discharge region. The anode — on the extreme right — is hollow, cooled in a similar manner as the cathode, and flanged to mate the monochromator. A Plexiglass flange is used to clamp the components together. It is grooved to locate the quartz disc such that the capillary aligns with the optical axis.

The source is operated at pressures in the vicinity of 1 torr. The applied potential is about 1000 volts, and the discharge current is 250 mA. The source may be operated at higher currents, with a corresponding increase in intensity, but the available power supply provides only 250 mA.

Figure 4 shows the intensity distribution of the dc light source operated with hydrogen. The most outstanding feature in the spectrum is the hydrogen resonance line (Lyman alpha) at 1215.7Å. However, the surrounding molecular spectrum is also emitted with useful intensities. Comparison of this emission spectrum with that produced by the argon spark source (see Figure 1) indicates that the intensities are of similar order of magnitude. Figure 5 shows the spectrum produced by the dc source, when it is operated with argon. In this case the argon resonance lines at 1048 and 1066Å are the principal features.

C. Sample Inlet System

Gas samples to be analyzed with the photoionization mass spectrometer are admitted to the ionization chamber via a Vactronics leak valve. Previously, most of the investigated gas mixtures were taken directly from steel cylinders and the sample source was connected directly to the mass spectrometer inlet valve. Since the cylinder pressure generally is considerably above the atmospheric pressure, contamination by air under these conditions was minimal. In the present study, the samples were prepared in 12-liter flasks at a final pressure slightly below one atmosphere, so that the gas line connecting the sample flask to the inlet valve had to be freed from air and other possible contaminants before the sample mixture could be studied. For this purpose, the gas inlet system was modified by the attachment of a glass tee to the high pressure side of the inlet valve, as shown in Figure 6. One branch of the glass tee led, via a stopcock to an auxiliary mechanical pump, while the other terminated in a tapered joint to which the sample flask was connected. In this manner, the line between the stopcock on the sample flask and

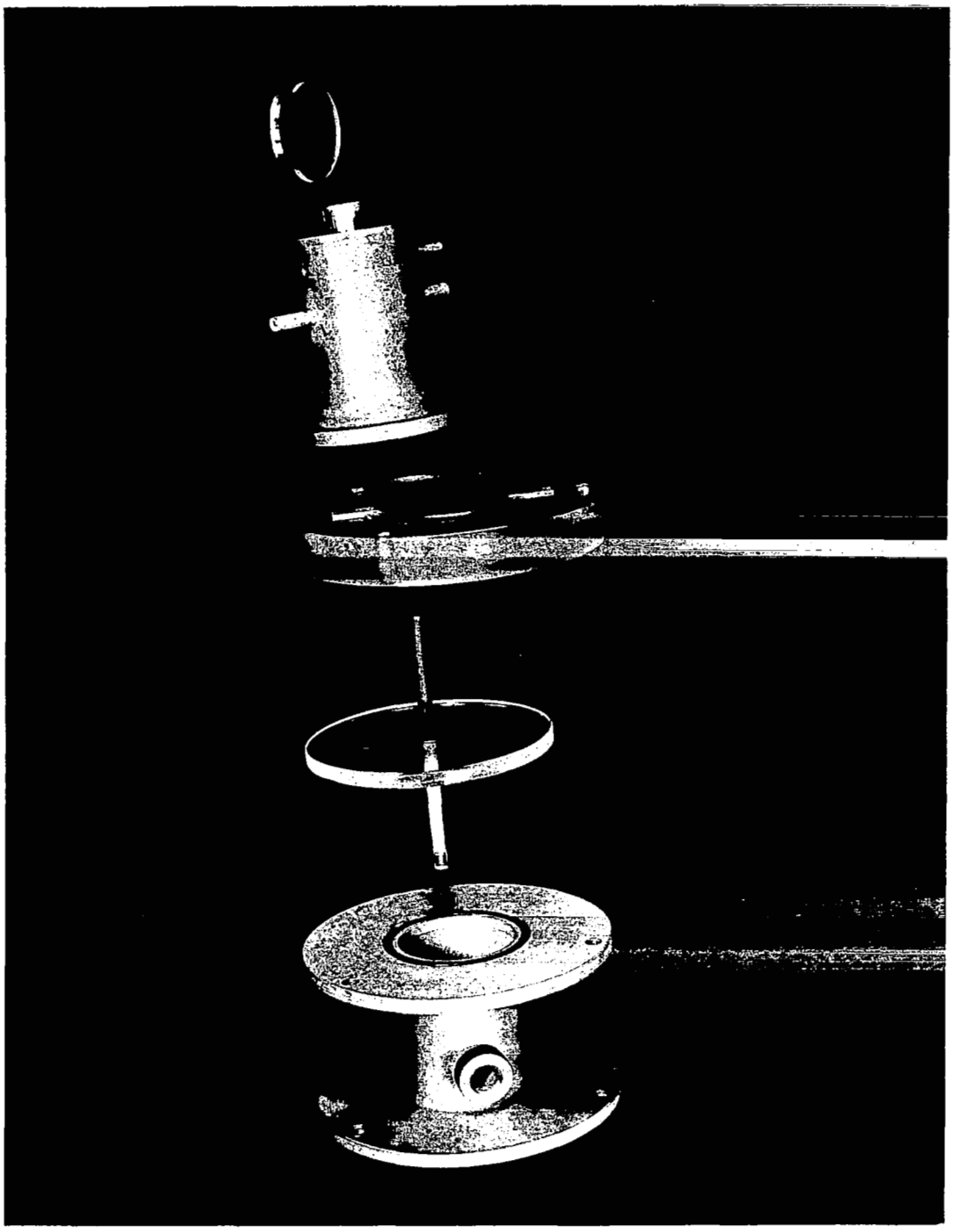

Figure 3. Components of dc source.

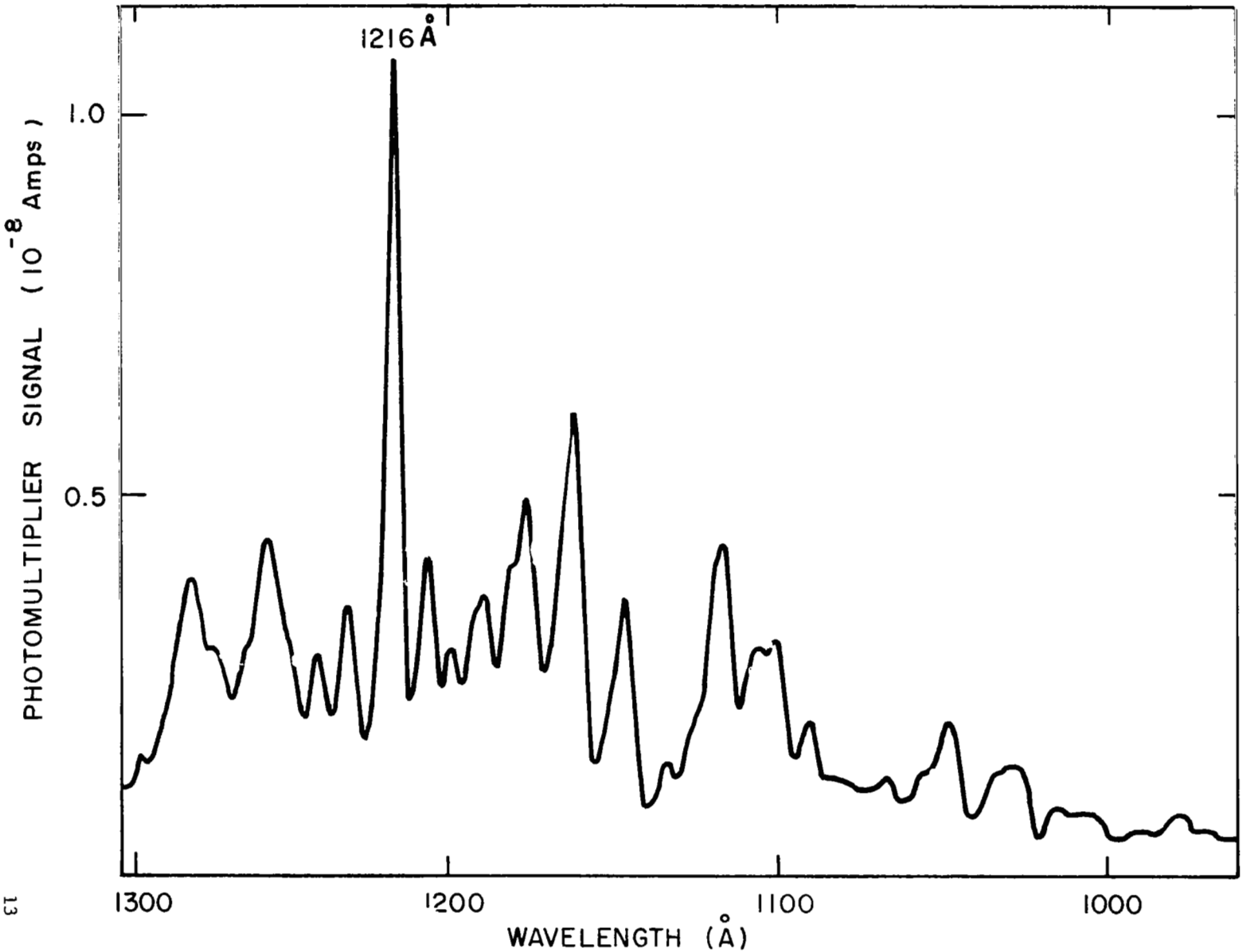

Figure 4. DC source spectrum, hydrogen.

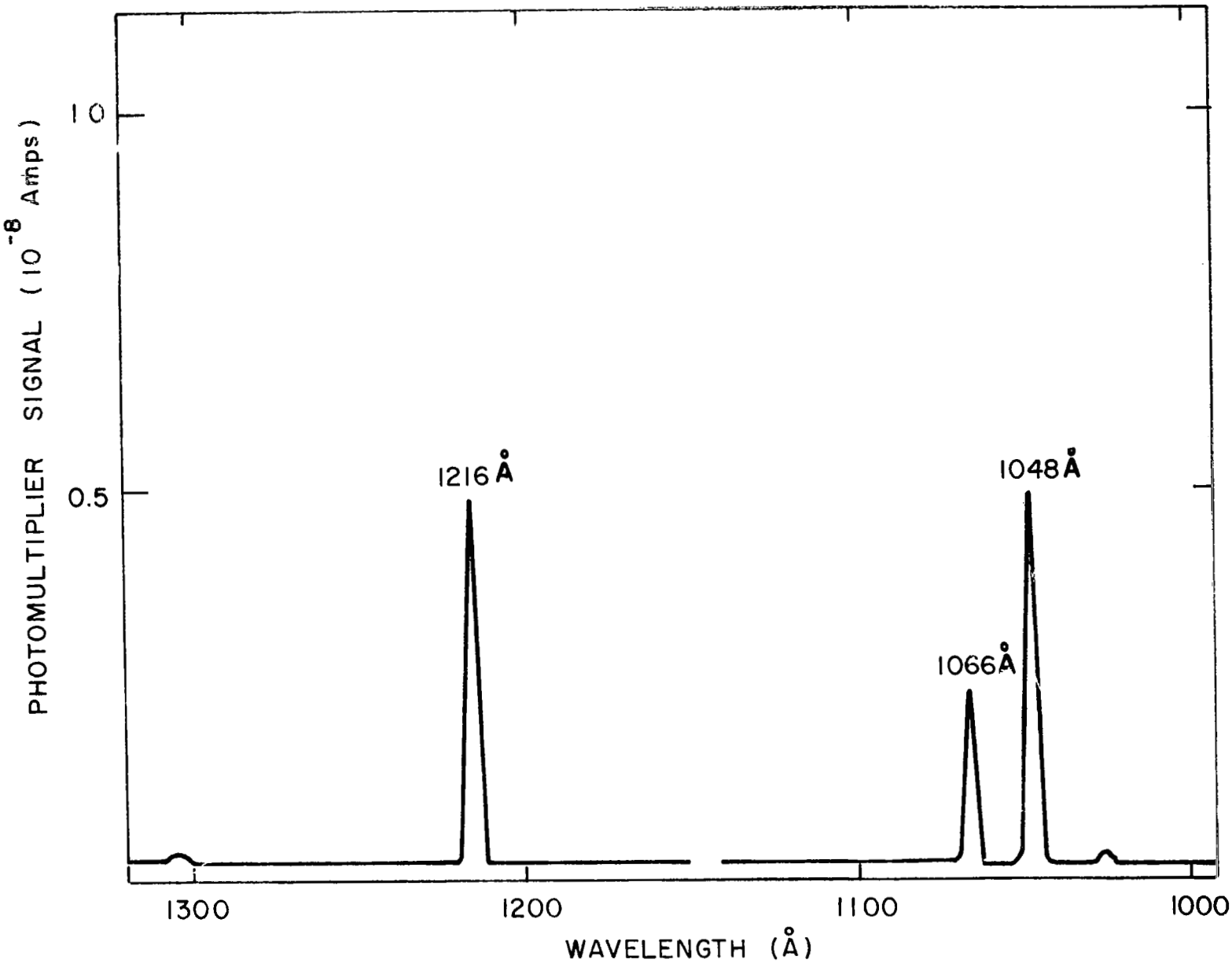

Figure 5. DC source spectrum, argon.

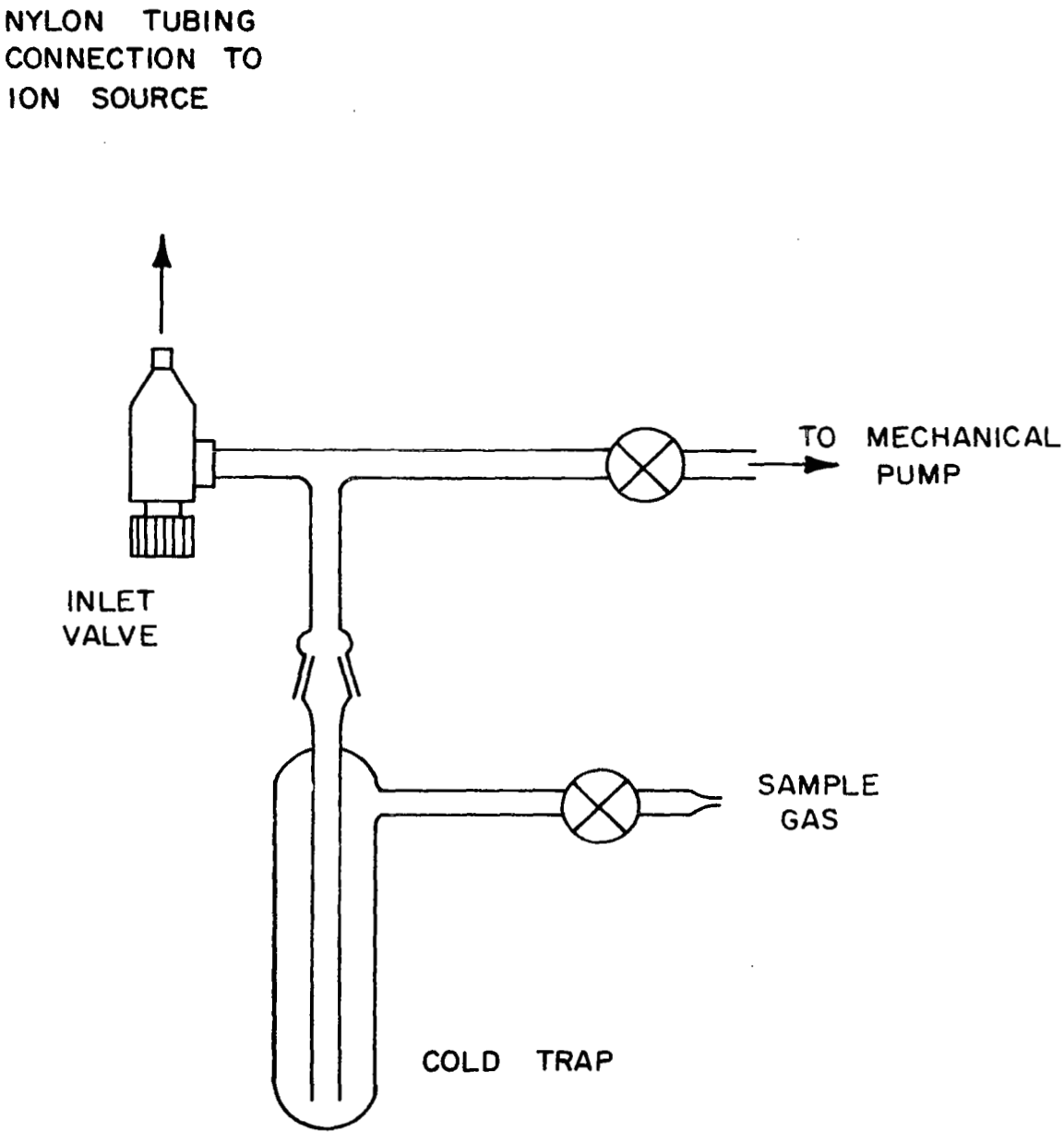

Figure 6. Sample inlet system.

the inlet valve could be evacuated before the sample flask was connected to the inlet valve and the sample admitted to the mass spectrometer ion source.

In some experiments, notably in the study of nitrogen dioxide, it became necessary to freeze the sample gas out in order that a check could be made on any non-condensable components still present. For this purpose, a cold trap fitted with a stopcock was attached to the tapered joint as shown in Figure 6, and the sample gas was admitted via the second stopcock. The trap was cooled either with liquid nitrogen or with a dry ice — acetone slurry, as required.

In addition to the described modification of the inlet system, it was found necessary to replace the inlet valve used previously, because the brass bellows were attacked by some of the more chemically agressive sample gases, such as NO_2 and $HC\ell$. Accordingly, the chrome plated brass valve was replaced by a similar unit made of stainless steel.

D. Sample Preparation

From Table 1, it is apparent that essentially all the substances investigated in this study have vapor pressures sufficiently high to allow the direct introduction into the ion source via the mass spectrometer inlet valve. However, for performing a comparative study of sensitivities the sample pressure in the ion chamber must be known. The determination of absolute pressures of most vapors and gases in the pressure domain 10 microns and below is difficult because the only available standard, the McLeod gauge, cannot be used with condensable gases. Other gauges show a significant variation in gauge sensitivity with the type of gas or vapor measured, so that they cannot provide a reliable absolute pressure determination. The thermocouple gauge used here to monitor the ion chamber pressure falls into that latter category. The range of this gauge is laid out for 0 to 100 microns, but it cannot be expanded so that it is not useful for pressures below 0.5 microns.

At sample gas pressures of ten microns or higher, the effect of ion-neutral interaction becomes important, resulting in the production of new ions which can alter the observed mass spectrum. Although for analytical purposes, the effect of ion reactions can be beneficial, it is strongly dependent on the sample gas pressure, so that the complexities of interpretation might be increased. Hence, high pressures of sample gas in the ion source were to be avoided in the present study whenever possible.

The most convenient procedure which circumvents the above difficulties consists of mixing a small concentration of the sample gas into an inert

carrier gas, and introducing the resulting gas mixture into the ion source. Then the response of the thermocouple pressure gauge is due essentially to that of the carrier gas. The gauge can be calibrated with respect to the carrier gas. In addition, the partial pressure of the sample in the ion chamber will be sufficiently low to minimize the occurrence of ion-neutral interactions.

In applying the outlined procedure, helium was selected as a convenient and inert carrier gas in many of those measurements which were aimed at determining the mass spectral fragmentation patterns and the sensitivities. Some experiments were performed using nitrogen as the carrier gas. Although it was realized that in view of the intended application of photoionization mass spectrometry to the analysis of cabin atmospheres the most appropriate carrier gas would be air, it was found and will be discussed later that in some cases the sample compound reacted with the oxygen and/or water vapor present in air. This effect was amplified in mixtures containing more than one compound. The presence of larger amounts of oxygen also causes interference of its signal at mass number 32 with those sample gases that develop a signal at the same mass number. On the other hand, helium and nitrogen do not ionize in the wavelength region investigated here ($> 800\text{Å}$), so that signal interference is not expected with these carrier gases. Nevertheless, with nitrogen a small signal was often observed at mass number 28, due to the incomplete blocking of wavelengths below 800Å by the argon filter when the argon spark source was employed. Hence, the use of nitrogen as a carrier gas was avoided whenever the sample compound was expected to produce a mass number 28 signal.

Mixtures of samples with the carrier gas were prepared in 12-liter round glass flasks. These were provided with a vacuum-tight stopcock, lubricated with the comparatively inert Kel-F grease. Also provided was a tube terminated by a stainless steel Swagelok fitting accommodating an inert elastomer septum. The flasks were connected to an auxiliary vacuum and gas handling manifold equipped with a diffusion pump to evacuate the flask to a pressure less than 1×10^{-3} torr. A mercury manometer isolated from the manifold by a cooled trap, was used to measure the pressure of all the permanent gases. Liquid substances were introduced to the flasks by means of a syringe injected through the elastomer septum.

The procedure for the preparation of sample carrier gas mixtures was as follows. Gases were taken from cylinders, and were introduced to the gas handling manifold via one or more detachable leak valves. The cylinder was connected to the valve inlet via a line of Tygon tubing. The line was flushed with the gas to be entered so that residual air and other impurities were driven out. The leak valve was closed, and attached to the manifold system. After evacuation of the system, the manifold was isolated from the vacuum pump, and the desirable amount of sample gas were metered in. Subsequently, the stopcock on the sample

flask was closed, the manifold was evacuated again and the carrier gas was introduced to the manifold through a second leak valve. The stopcock to the sample flask was then re-opened and more carrier gas added until the pressure in the system was close to one atmosphere. The percentage of sample in the flask was calculated from the known partial and total pressures.

Liquid samples were injected into the evacuated and isolated sample flask. Then, the carrier gas was added as described above. Since the partial pressures of the liquid samples could not be measured directly, they had to be calculated from the known volume of the flask, the injected volume of sample liquid, and the density of the liquid at the ambient temperature. To avoid the condensation of liquid inside the flask, it was important that the equilibrium vapor pressures of the substances at room temperature were not exceeded. The upper limit of the permissible sample size that could be injected was calculated and is given in Table 1. Despite precautions, condensation was observed in mixtures. In these cases, the sample size was reduced until condensation was absent.

Most of the compounds listed in Table 1 were available commercially with research grade purity. The only exception was formaldehyde. This gas can be handled only at low pressures, because it polymerizes easily. Formaldehyde was prepared from its trimer paraformaldehyde which was purchased as a fine powder. Paraformaldehyde was placed in a bulb attached to the gas handling manifold and the system was evacuated. The bulb was heated gently until gas formation occurred. The formaldehyde developed in this manner was collected in a trap cooled with liquid nitrogen. A portion of it was distilled into a 12-liter sample flask, the gas pressure was measured with the manometer, and helium was added as the carrier gas.

Phenol, although commercially available, presented a problem in that it is crystalline and its room temperature vapor pressure is lower than that of all the other compounds. Initially, a sample was prepared by injecting heated molten phenol into a sample flask, admitting helium subsequently. Since no mass spectrum could be obtained from this sample, a few phenol crystals were placed into a small bulb which was attached directly to the inlet system and was evacuated. Also with this procedure, which should result in a sufficient pressure of phenol in the ion source, no mass spectrometer signals could be detected. It was concluded that phenol was absorbed on its way to the ion source, and no further attempts were made to record its mass spectrum. In the list of compounds to be investigated, phenol was substituted by propionaldehyde.

E. Operational Procedures

The instrument was kept evacuated at all times, except when servicing became necessary. Overnight, and during periods when not in use,

the mechanical pumps were kept operating, but the three valves connecting the fore line to the three diffusion pumps were closed and the diffusion pumps were switched off. All other valves were kept closed. Particular attention was paid to keep the monochromator entrance slit valve closed between measurements, even when the diffusion pumps were operating, in order that oil vapor from the mechanical pump serving the light sources did not enter the monochromator, because oil deposition on the grating would decrease its efficiency. The back diffusion of oil vapor is minimized when a gas flow is established. Another reason for keeping the monochromator entrance slit valve closed between measurements is the deposition on the grating of debris emitted from the spark light source. The deposition of sputtered material on the surface of the grating also causes a decrease in its efficiency.

The start-up procedure entails first opening the valve on diffusion pump #1 underneath the monochromator, then opening the other two diffusion pump valves. Evacuating first the monochromator prevents an adverse pressure differential across the monochromator exit slit assembly. The monochromator entrance slit valve must be closed during the pumping stage or the baffles making up the gas filter will be propelled against the grating by inrushing air. After evacuation by the main mechanical pump, the water flow provided to cool the diffusion pumps should be checked. Then, diffusion pumps may be switched on. It will take between 30 and 60 minutes to establish the required vacuum (2×10^{-6} torr or better in the magnetic analyzer section). During this time, operation of the light source can be initiated. The desired light source, either the argon spark source or the dc source, is attached to the differential pumping flange at the monochromator entrance arm. A vacuum tight seal is accomplished with an O-ring compressed by three bolts. The gas line, water lines and power lines are connected. The vent valve at the differential pumping section is closed and the second mechanical pump is switched on to evacuate the light source section.

After connection of a gas storage tank to the light source gas inlet valve, the valve is opened, a gas flow is established, and the valve is adjusted to provide the desired pressure in the light source. The power supply and the spark gap (only for the spark source) are switched on. Water cooling of the light source must be established before the power supply is activated. Then the voltage can be increased until the discharge strikes and the appropriate current level is achieved.

When the analyzer section pressure has dropped to a value of 5×10^{-6} torr or better, the remaining power supplies and electronic equipment can be switched on. The magnet supply should be adjusted to low currents, so long as the magnet is not cooled. Otherwise the magnet coils may overheat.

The instrument is now ready for operation. The monochromator entrance slit valve may be opened, and the photomultiplier should register a signal. The wavelength drive may be activated to turn the grating

to a suitable spectral line, or to take a spectrum of the light source as a check on its spectral output. It should be noted that the gas line of the light source may initially contain air and that flushing by the employed gas may take some time. When the photomultiplier signal shows that the light flux has reached a stable level, a gas sample can be connected to the mass spectrometer inlet system. The inlet valve is opened until a pressure of the order of one micron is reached in the ion source. The zero lock of the Keithley electrometer is opened and the instrument is put onto a suitable current scale (1×10^{-12} - 3×10^{-10} amperes). A mass spectrum is taken by means of the magnet current sweep unit.

The range and values of operating conditions that are in line with the outlined procedure and have been found convenient are summarized in Table 3. Some additional comments may be of value: (a) the light intensity generated by the dc light source increases with the current, whereas that of the spark source increases with the square of the voltage. However, the discharge currents should not exceed 300 mA for the dc source, and 85 mA for the spark source, (b) the stability of the spark light source decreases when the tungsten points of the spark gap deteriorate. Periodic replacement of the points is recommended, (c) the photomultiplier supply voltage is low compared with standard values, but due to the pulsed operation, the spark source produces high instantaneous signals which can saturate the photomultiplier electronic circuit. The low supply voltage was chosen to avoid such saturation in order that the averaged anode current registered by the microammeter be proportional to the light signal, (d) because of the residual magnetization of the analyzer magnet, the mass scale will not be exactly proportional to the square of the magnet current. This effect may be enhanced if the magnet current is swept back and forth over a larger range. However, a good reproducibility of the mass scale is achieved if the current sweep is operated only in one direction. In the present work the scan direction was always from higher to lower currents.

TABLE 3

PHOTOIONIZATION MASS SPECTROMETER OPERATING CONDITIONS

1. Instrument Pressures

monochromator: 2×10^{-4} torr without gas filter, up to 20 microns with gas filter

(If pressure is too high, the electron deflector will arc and the acceleration power supply will shut off.)

ion source: Background pressure not measurable. Upon sample introduction, the pressure is typically 1 micron. Pressure can be increased if necessary.

mass analyzer: 2×10^{-6} torr or better.

2. Spark Light Source

Type of gas: Argon
Source pressure: 150-200 microns
Operational current: 50-70 mA

3. DC Light Source

Type of gas: Argon; Argon-hydrogen mixture
Source pressure: 200-2000 microns
Current setting: 250 mA

4. Monochromator

Slit setting: about 0.25 mm
Wavelength range: 800-1300Å
Resolution: 3-5Å half width

5. Photomultiplier Detector

Supply voltage: 600 volts
Microammeter set to: 3, 10 or 30 $\times 10^{-9}$ ampere full scale

6. Ion Acceleration

Power supply set to: 500-1000 volts, as high as is compatible with the desired mass range.

Focusing controls adjusted to maximum ion signal.

TABLE 3

(continued)

7. Magnetic Analyzer

For current sweep set voltage and current controls to maximum (36 volts, 10 amperes), then use the programmer to sweep towards lower current. For controlled current, set voltage control and programmer to maximum, then adjust current control to desired current (and mass number).

8. Detector and Readout

Electron multiplier supply: 300 volts
Electrometer scale setting: 1×10^{-12} - 3×10^{-10} amps full scale.

III. RESULTS

A. General

The principal aim of the present investigation was to determine for the substances listed in Table 1 their fragmentation patterns and mass spectrometric sensitivies as a function of ionizing wavelength. Clearly, a detailed wavelength response of each substance is not required for an assessment of the analytical potential of photoionization mass spectrometry, but the trend should be made apparent. In the present study, therefore, measurements were made at four wavelengths which were selected such that the associated energy differences were about 1.5 eV. The exact choice of ionizing wavelengths was dictated mainly by the availability of strong emission lines in the spectra generated by the light sources. Accordingly, the following emission lines were used: 803, 950, 1048 and 1216Å, each isolated with the monochromator with a characteristic resolution at half peak height of 3.5Å. The energies in electron volts represented by these ionizing wavelengths are 15.42, 13.02, 11.80, and 10.20 eV, respectively. The two lines at the lower wavelengths were generated with the argon spark light source; the 1048Å argon resonance line was obtained with the dc light source operated with argon; and the 1216Å Lyman-alpha line was produced with the dc light source operated with a mixture of argon and hydrogen.

The following sections will first present the mass spectral fragmentation patterns observed for the individual compounds, then the associated sensitivities and detection limits. Subsequently, results for five mixtures of three or more components will be given.

B. Mass Spectra

The observed mass spectra and relative peak abundances of the investigated compounds are compiled in Table 4 for each of the employed ionizing wavelengths. The last column shows, for comparison, relative abundances of the six strongest peaks obtained by impact of 70 eV electrons, as taken from the Index of Mass Spectral Data (Ref. 7). For the butyl alcohols more complete electron impact abundance data were available from other sources (Ref. 8) and are included accordingly.

The development of the fragmentation pattern with increasing ionization energy is apparent in practically all cases. At the longest ionizing wavelength, i.e. the lowest ionizing energy, the spectra consist mainly of the parent peak, and if other ions are produced, the parent peak is usually the strongest feature in the spectrum. Exceptions are secondary butyl alcohol and ethylene dichloride for which the fragment

TABLE 4

MASS SPECTRA OF INVESTIGATED
COMPOUNDS AT FOUR IONIZING WAVELENGTHS

COMPOUND	m/e	IONIZING WAVELENGTH (Å)				ELECTRON IMPACT
		1216	1048	950	803	70 eV
Acetone	58	100	100	100	29	23
	43		23	100	100	100
	42					7
	29					4
	27					8
	26					6
Acetaldehyde	45		19	14	10	
	44		100	100	94	88
	43		23	53	68	50
	42				3	
	41					6
	31			1	2	
	29			27	100	100
	28				1	9
	27				1	
	26					6
	16			1	11	
	15			1	40	
	14				1	
Allyl Alcohol	59	3	2	1	2	
	58	100	31	20	24	27
	57	12	100	100	100	100
	55				3	
	41			3	5	
	40		2	5	9	
	39			1	13	40
	31		1	2	25	60
	30		8	6	12	
	29		1	9	45	80
	28		2	6	17	
	27				7	45
	26				1	
Ammonia	18	33	4	10	9	1
	17	100	100	100	100	100
	16					80
	15					8
	14					2

CK-1589

TABLE 4 (continued)

COMPOUND	m/e	IONIZING WAVELENGTH (Å)				ELECTRON IMPACT
		1216	1048	950	803	70 eV
Benzene	78	100	100	100	100	100
	77				16	14
	52					19
	51					19
	50					16
	39					14
Butene-1	56	100	100	100	100	39
	55			5	4	18
	54				12	
	41				5	100
	39			12	15	38
	28					27
	27					25
cis-Butene-2	56	100	100	89	73	51
	55		20	68	73	23
	41		30	100	100	100
	39				17	37
	28				9	31
	27				16	34
trans-Butene-2	56	100	100	80	66	50
	55		19	64	69	23
	41		27	100	100	100
	39				17	37
	28				9	31
	27				16	34
n-Butyl Alcohol	74	100	8	2	2	1
	73			3	3	
	70			2	3	
	61			2	3	
	59			1.4	1.6	
	58				1	
	57		5	19	22	7
	56	71	100	100	100	85
	55		2	12	19	12
	45			2	7	
	44			1.6	4	
	43		5	35	74	59
	42		12	19	27	31
	41		5	20	54	60
	40				2	

TABLE 4 (continued)

COMPOUND	m/e	IONIZING WAVELENGTH (Å)				ELECTRON IMPACT
		1216	1048	950	803	70 eV
n-Butyl Alcohol (continued)	33		5	5	9	9
	32			3	6	
	31		7	21	58	100
	29			1	10	30
	28			2	8	16
	27				8	52
	19				1.6	
	18			1.5	4	
iso-Butyl Alcohol	74	100	45	30	19	9
	73			5	3	
	59		2	5	4	5
	57		11	9	8	4
	56		13	9	6	3
	55			3	6	4
	45			1	1.5	
	44		5	5	5	
	43		29	100	100	100
	42		60	79	63	57
	41			8	47	56
	33		100	84	60	53
	32			4.5	5	
	31			15	34	63
	29				4	
	28				1.7	
	27			1	10	43
	18			8	8	2
sec-Butyl Alcohol	74	28	3	2	1	
	73		2	3	2	
	70		2			
	61		2	1	1	
	60		2			
	59	11	40	24	22	18
	58		2	1	1	
	57		2	6	11	3
	56		2	2	2	1
	55			1	3	2
	46		2	2	2	
	45	5	100	100	100	100
	44	100	44	13	13	
	43			4	8	10
	41			5	9	11

TABLE 4 (continued)

COMPOUND	m/e	IONIZING WAVELENGTH (Å)				ELECTRON IMPACT
		1216	1048	950	803	70 eV
sec-Butyl Alcohol (continued)	32			1	2	
	31			5	12	21
	29				3	15
	27				1	17
	19				2	
	18			1	2	
tert-Butyl Alcohol	74					
	60	4	4	4	4	3
	59	100	100	100	100	100
	57		4	10	16	9
	56				1	2
	55				2	2
	43				4	14
	42					3
	41			2	18	21
	32				1	8
	31			5	32	36
	29				4	13
	18				1	10
Carbon Disulfide	78					9
	77					3
	76	100	100	100	100	100
	64					1
	44					18
	32				13	22
1,4-Dioxane	88	100	100	94	30	31
	58	1	71	77	22	24
	31			5	10	17
	29			15	22	37
	28			100	100	100
	15					17
Ethyl Acetate	88/89	100	100	59	2	7
	87		72	50	5	
	73		16	9	1	
	70		80	47	10	10
	61		48	40	9	10
	45		21	27	11	15
	44			4	4	
	43		7	100	100	100
	42			1	1	
	29			8	10	13

TABLE 4 (continued)

COMPOUND	m/e	IONIZING WAVELENGTH (Å)				ELECTRON IMPACT
		1216	1048	950	803	70 eV
Ethylene Dichloride	102		8	8	9	
	100		58	48	40	
	98		78	75	65	
	65		5	23	10	
	64		42	37	26	32
	63		14	59	35	19
	62		100	100	73	100
	61				9	
	51			7	21	
	49			17	62	38
	27			5	100	92
	26					32
Formaldehyde	32			5	6	
	31		4	3	4	
	30		100	100	75	
	29			41	100	
	28			1	3	
	18			3	6	
Freon 11	121				1	
	119				3	
	117				3	
	105		10	13	11	11
	103		57	71	64	63
	101		100	100	100	100
	66					14
	47					10
	35					11
	31					10
Hydrogen Chloride	39			5	4	
	38			32	32	32
	37			11	11	5
	36			100	100	100
	35					17
Hydrogen Sulfide	36		4	5	5	4
	35		3	3	5	2
	34		100	100	100	100
	33				48	42
	32			2	42	44
	1					5

TABLE 4 (continued)

COMPOUND	m/e	IONIZING WAVELENGTH (Å)				ELECTRON IMPACT
		1216	1048	950	803	70 eV
Methane	17			6	6	2
	16			100	100	100
	15				75	86
	14					16
	13					8
	12					3
Methyl Alcohol	33		12	22	26	1
	32		100	100	64	72
	31		11	97	100	100
	30			6	2	8
	29					42
	28					9
	18					2
Methylene Chloride	88		11	10	9	
	87		5	3	4	
	86		64	61	62	36
	85		11	8	10	
	84		100	96	97	58
	83		10	9	12	
	51			32	31	30
	50			1	2	
	49			100	100	100
	48			2	3	
	47					18
	35					12
Nitric Oxide	30	100	100	100	100	100
Nitrogen Dioxide	47					1
	46	100	100	100	100	37
	30			20	39	100
	16					22
	14					10
Propionaldehyde	59	17	24	25	29	
	58	100	100	100	62	39
	57		17	55	35	15
	44			2	2	
	43			3	3	11
	31				3	
	30			10	6	
	29		4	55	100	100
	28			56	65	69
	27				12	55
	26					19
	15				1	

TABLE 4 (continued)

COMPOUND	m/e	IONIZING WAVELENGTH (Å)				ELECTRON IMPACT
		1216	1048	950	803	70 eV
Sulfur Dioxide	66				6	5
	64			100	100	100
	50					2
	48					49
	32					10
	16					5
Toluene	92	100	100	100	54	73
	91			78	100	100
	65					11
	63					9
	51					8
	39					15
Vinyl Chloride	64	30	34	34	32	25
	63	3	3	4	4	
	62	100	100	100	100	83
	61				3	
	35					9
	28			1	1	37
	27			24	54	100
	26			1	5	34
	25					13
m-Xylene	106	100	100	64	50	64
	105			8	31	28
	92	10	14	18	11	
	91		48	100	100	100
	77					13
	51					15
	39					19
o-Xylene	106	100	100	67	47	58
	105			11	26	24
	92	9	14	15	10	
	91		49	100	100	100
	77					13
	51					16
	39					16
p-Xylene	106	100	100	85	48	64
	105			10	36	30
	92	18	31	8	9	
	91		51	100	100	100
	77					14
	51					16
	39					39

peak intensity exceeds that of the parent peak even at the highest compatible ionizing wavelength, and tertiary butyl alcohol and freon 11, which show no parent peak at all. Only a few substances exhibit no fragmentation throughout the investigated wavelength range. These are ammonia, nitric oxide and sulfur dioxide. Many of the spectra obtained show a quite sizable contribution to the parent plus one peak. In some cases, this may be due to isotopes, such as C^{13} whose concentration is about 1 percent. However, in other cases the M+1 peak is too strong to be caused by isotope contributions. For example, ammonia falls into this category. In these cases, the M+1 peak is probably caused by hydrogen or proton transfer following ion-neutral interactions. Thus the strong M+1 peak observed with ammonia is due to the ion NH_4^+, formed as a consequence of the strong dipole interaction in ammonia. A similar observation is made with ethyl acetate. In this case, the parent and the M+1 peak cannot be fully resolved and their abundances were lumped together for the purpose of presentation in Table 4.

Most of the substances show essentially fully developed fragmentation patterns at 803Å. For example, the mass spectrum of 1,4 - dioxane at 803Å is very similar to that obtained with electron impact ionization. Apparently, the increase in energy from 15.4 to 70 eV does not result in a significant change in the ion fragmentation processes for many compounds. This observation indicates that for analytical applications of photoionization mass spectrometry there is no advantage in lowering the ionizing wavelength below 800Å. On the contrary, the fragmentation patterns suggest that the optimum wavelength range is 950 to 1216Å. Light in this wavelength region ionizes most substances with a minimum of fragmentation, yet the mass spectra are sufficiently developed to allow the recognition of a pattern so that use can be made of strong features other than the parent peaks for analytical assessments.

For the recognition of mass spectral patterns and for analytical applications, it is important to know the degree of reproducibility provided by the instrument in this respect. This factor can be determined by measurements of isotopic abundances. Most isotope abundances are too small to be useful in the present context because of the limited sensitivity of the instrumentation. However, the chlorine isotopes $C\ell^{35}$ and $C\ell^{37}$ have natural abundances of 75.5 and 24.5 percent respectively. Their ratio, approximately 3.1 to 1, is of a magnitude which can be checked conveniently using the appropriate peaks of the chlorine containing compounds. These are ethylene dichloride, freon 11, hydrogen chloride, methylene chloride and vinyl chloride. Table 5 shows, for these compounds, the relative abundances of the observed peaks for the four ionizing wavelengths employed, the ions causing the signals, and the relative abundances calculated from the known natural abundances of the two chloride isotopes. The experimental results indicate that the calculated abundances are reproduced to better than 2 percent of the total and that the least abundant mass peaks show a deviation of less than 20 percent from the average. There appears to be no dependence on wavelengths. The averaged measured abundances for each ion are in excellent

TABLE 5

RELATIVE ABUNDANCE OF MASS PEAKS DUE TO $^{35}C\ell$ AND $^{37}C\ell$ IN THE MASS SPECTRA COMPOUNDS CONTAINING CHLORINE

COMPOUND	m/e	ASSIGNMENT	RELATIVE ABUNDANCE Experimental Results					CALCULATED
			1216Å	1048Å	950Å	801Å	Average	
Ethylene dichloride	102	$C_2H_4{}^{37}C\ell{}^{37}C\ell^+$	-	0.06	0.06	0.08	0.07	0.06
	100	$C_2H_4{}^{37}C\ell{}^{35}C\ell^+$	-	0.39	0.37	0.35	0.37	0.37
	98	$C_2H_4{}^{35}C\ell{}^{35}C\ell^+$	-	0.54	0.57	0.56	0.56	0.57
	65	$C_2H_4{}^{37}C\ell^+$	-	0.263	0.281	0.223	0.255	0.245
	63	$C_2H_4{}^{35}C\ell^+$	-	0.736	0.721	0.778	0.745	0.755
	64	$C_2H_3{}^{37}C\ell^+$	-	0.296	0.270	0.263	0.276	0.245
	62	$C_2H_3{}^{35}C\ell^+$	-	0.705	0.730	0.738	0.724	0.755
Freon-11	105	$CF^{37}C\ell{}^{37}C\ell^+$	-	0.06	0.07	0.06	0.06	0.06
	103	$CF^{37}C\ell{}^{35}C\ell^+$	-	0.34	0.39	0.37	0.37	0.37
	101	$CF^{35}C\ell{}^{35}C\ell^+$	-	0.60	0.54	0.57	0.57	0.57
Methylene chloride	88	$CH_2C\ell{}^{37}C\ell{}^{37+}$	-	0.06	0.06	0.05	0.06	0.06
	86	$CH_2C\ell{}^{37}C\ell{}^{35+}$	-	0.36	0.36	0.37	0.36	0.37
	84	$CH_2C\ell{}^{35}C\ell{}^{35+}$	-	0.58	0.58	0.58	0.58	0.57
	51	$CH_2{}^{37}C\ell^+$	-	-	0.243	0.237	0.240	0.245
	49	$CH_2{}^{35}C\ell^+$	-	-	0.757	0.763	0.760	0.755

TABLE 5 (continued)

COMPOUND	m/e	ASSIGNMENT	RELATIVE ABUNDANCE Experimental Results					CALCULATED
			1216Å	1048Å	950Å	801Å	Average	
Hydrogen chloride	38	$H^{37}C\ell^+$	-	-	0.243	0.243	0.243	0.245
	36	$H^{35}C\ell^+$	-	-	0.757	0.757	0.757	0.755
Vinyl chloride	64	$C_2H_3{}^{37}C\ell^+$	0.231	0.254	0.254	0.243	0.246	0.245
	62	$C_2H_3{}^{35}C\ell^+$	0.769	0.746	0.746	0.757	0.754	0.755

agreement with the calculated ones. It can be concluded, that the reproducibility of mass spectral patterns as judged from the isotopic abundances is comparable to that of other common mass spectrometers which are not specifically instrumented for isotopic abundance analyses.

As pointed out in the introduction, one aspect of the present study is the investigation of a differentiation of isomeric structures by means of their fragmentation patterns. This aspect will now be discussed. Among the investigated substances are three structural isomers: the butenes, the butyl alcohols, and the xylenes. A comparison of their mass spectral patterns provides the following information. The mass spectral patterns (and relative peak heights) of cis- and trans-butene are essentially identical at all the four ionizing wavelengths employed. The characteristic feature of the corresponding fragmentation patterns is that the predominant peak changes from the parent peak at m/e = 56 at the longer wavelengths to the fragment ion peak at m/e = 41 at 950Å and 803Å. This is not the case for butene-1, for which the parent ion remains the most intense ion at all wavelengths. Butene-1 does not produce a fragment ion peak at m/e = 41 at 1048 or 950Å, whereas cis-and trans-butene do. Consequently, it is possible to differentiate between cis- and trans-butene-2 on one hand, and butene-1 on the other by means of their different fragmentation patterns in a limited wavelength range. It is interesting to note that electron impact ionization does not provide sufficiently different fragmentation patterns for the three butenes to allow a similar discrimination.

In contrast to the results obtained for the butenes, no appreciable differences can be discerned for the mass spectra of the three xylenes. Both the spectra and the ion intensities observed for ortho-, meta-, and para-xylene are very similar, so that a differentiation between these isomers by means of their fragmentation patterns is precluded. In this case, therefore, no advantage is provided by photoionization compared to electron impact ionization.

The fragmentation patterns of the four butyl alcohols exhibit considerable differences, so that there is no difficulty in discriminating between the different butyl alcohol isomers. In a later section of this report, the analysis of a mixture of the four butyl alcohols will be described. It should be noticed, however, that the butyl alcohol fragmentation patterns produced by electron impact ionization are also quite different, so that electron impact ionization also provides discrimination. The advantage of photoionization in this case is mainly the greater simplicity of the mass spectra so that the analysis is facilitated. Again, the 1048 to 1216Å wavelength region is more favorable for analytical applications than the wavelength region below 950Å where the fragmentation is extensive and the resulting mass spectra are complex.

Finally, it may be of interest to compare the mass spectra of functional isomers. The group of substances including allyl alcohol proprionaldehyde and acetone may serve as an example. The parent peaks of these compounds fall together at m/e = 58, so that their discrimination can be provided only by differences in the fragmentation patterns. A previous technique of discrimination which has been employed in the similar case of acetone-butane mixtures made use of the differences in the

ionization thresholds so that differentiation was achieved by a choice of ionizing wavelength. Under appropriate conditions, acetone was ionized whereas butane was not. This technique is not applicable in the case of acetone and allyl alcohol because their ionization potentials (and photoionization onsets) coincide. The fragmentation patterns of acetone, allyl alcohol and proprionaldehyde are sufficiently different to permit discrimination between the three compounds if the ionizing wavelength is 1048Å or lower. Results for a mixture of these components will be discussed in a subsequent section.

The results described in this section can be summarized briefly as follows. Photoionization produces simpler mass spectra when compared with electron impact, provided the ionizing wavelength lies in the wavelength region above 950Å. Sufficient fragmentation occurs in most cases to permit discrimination between those substances that have coinciding parent peak mass numbers, i.e. between functional isomers. In some cases, the fragmentation patterns are sufficiently different also for structural isomers to allow their discrimination. This is so for butene-1 compared with cis- and/or trans-butene, and for the various butyl alcohols, but not for ortho-, meta-, or para-xylene. Isotope abundances, measured for the two chlorine isotopes, reflect rather faithfully the natural abundance ratio. No dependence of the abundances on ionizing wavelength has been noted.

C. Sensitivities

An important factor in the analytical application of the photoionization mass spectrometer is the sensitivity of the instrument with respect to the gases or vapors to be investigated. Accordingly, the mass spectrometric sensitivity was determined for each of the individual substances whose fragmentation patterns were studied at the employed four ionizing wavelengths.

The sensitivity of a mass spectrometer commonly is given in the units amperes/torr, corresponding to the ratio of the readout current to the pressure in the ion source, assuming that the ion production is linear with pressure. This convention will be adopted here. The assumption that the ion current is proportional to the pressure holds only within a limited pressure range, because of the occurrence of ion-neutral reactions on one hand and nonlinear light absorption on the other at higher ion source pressures. By the use of a carrier gas in the present investigation it has been attempted to minimize the influence of ion-molecule reactions. Nonlinear light absorption occurs only at pressures greater than 100 microns, which is beyond the range of pressure used during the experiments. Up to 10 microns pressure, it was found that ion currents were indeed proportional with the pressure unless extensive ion-molecule interaction occurred.

The signal current produced at the anode of the electron multiplier detector is given by

$$j = G \gamma e \sigma n \ell I$$

where I is the intensity of ionizing light (in photons/sec.), ℓ is the effective length of the ion chamber, n is the gas density of an ionizable component, σ is the photoionization cross section, e is the electron charge, γ is the efficiency with which ions are extracted from the source and directed into the mass analyzer, and G is the gain provided by the electron multiplier and includes any losses of ion current in the mass analyzer. Since the gas density is proportional to the pressure (at room temperature $n = 3.3 \times 10^{16} p$), the sensitivity is

$$S = j/p = G \gamma \epsilon \sigma I$$

where for convenience, the substitution $\epsilon = 3.3 \times 10^{16}$ eℓ has been made. Accordingly, if the collection efficiency and the gain of the electron multiplier, i.e. the instrumental factors, remained constant, the sensitivity for a given fragment ion would depend only on the photoionization cross section and the intensity of the ionizing radiation. This ideal situation cannot be expected to apply in practice. For example, the collection efficiency depends critically on the applied electric fields, the repeller setting, the acceleration voltage, the focusing conditions, etc. The gain of the electron multiplier depends on the applied voltage, the age and/or the surface contamination of the dynodes, and other possible factors. It is unrealistic to expect all of these parameters to remain constant over long periods of time. Accordingly, it was required to check on the change of the sensitivity from time to time with the aid of a standard gas and to determine sensitivities relative to the standard. In the present work, nitric oxide was employed as the standard, because it ionizes at all four wavelengths used and the only ion formed even at 803Å is the parent ion NO^+. The importance of this procedure became apparent when the instrument developed a leak after the investigation had been about half-way completed. Locating and fixing the leak required a temporary removal of the ion source which resulted in a loss of sensitivity by about a factor of 5, presumably due to problems in re-aligning the ion source plates. The relative sensitivities with respect to NO remained unaffected as shown by duplicate runs involving several compounds.

Relative sensitivities for all the investigated compounds are assembled in Table 6. In each case sensitivities are given for the parent peak (unless this ion peak is absent), and the strongest peak in the mass spectrum if this is not the parent peak. In addition, the concentration of sample in the carrier gas and the applied acceleration voltage are indicated. The sensitivity data are normalized with respect to the light intensity and the ion acceleration potential, assuming the other parameters to remain constant. Thus the relative sensitivities given in Table 6 are

$$S_r = \frac{S_1}{S_2} \frac{I_2}{I_1} \frac{\gamma_2}{\gamma_1}$$

where the subscripts 1 and 2 refer to the sample compound and nitric oxide, respectively.

TABLE 6

RELATIVE SENSITIVITIES (WITH REFERENCE TO NO)
AT FOUR WAVELENGTHS

COMPOUND	CONCENTR. IN CARRIER GAS	ACCELER. VOLTAGE	MASS NO	IONIZING WAVELENGTH (Å)			
	%		amu	803	950	1048	1216
Acetone	7.0	900	58	0.25	1.00	1.37	5.4
			43	0.86	1.00	0.31	-
Acetaldehyde	10	900	44	0.45	0.72	1.74	-
			29	0.48	0.19	-	-
Allyl Alcohol	2.9	900	58	0.01	0.05	0.75	1.8
			57	0.05	0.25	2.50	-
Ammonia	9	900	17	0.46	0.61	0.55	0.033
Benzene	8.5	500	78	0.17	0.67	6.1	7.8
Butene-1	7.8	900	56	0.81	2.30	5.56	2.82
cis-Butene-2	9	900	56	0.43	1.94	2.00	3.10
			41	0.59	2.18	-	-
trans-Butene-2	8.5	900	56	0.43	1.94	2.10	4.74
			41	0.65	2.40	-	-
n-Butyl Alcohol	0.82	600	74	0.078	0.32	0.132	0.24
			56	2.60	10.00	1.65	0.17
iso-Butyl Alcohol	1.4	600	74	0.21	0.42	0.52	0.55
			33	0.66	1.18	1.15	-
			43	1.10	1.40	0.33	-
sec-Butyl Alcohol	2.1	600	74	0.27	0.30	0.04	0.21
			44	0.99	5.30	0.44	0.75
			45	9.00	10.00	1.00	0.037
tert-Butyl Alcohol	2.4	600	74	-	-	-	-
			59	2.7	5.4	3.3	2.10
Carbon Disulfide	5.5	700	76	4.0	8.1	31.0	4.80
1,4 Dioxane	3	600	88	0.027	0.097	0.72	1.52
			28	0.091	0.10	-	-
Ethyl Acetate	7	600	88	0.0087	0.063	0.41	0.44
			43	0.097	0.118	0.016	-
Ethylene Dichloride	7.4	550	98*	0.14	0.20	0.23	-
			62	0.18	0.27	0.26	-
			27	0.22	0.013	-	-
Formaldehyde	1.9	900	30	1.10	3.00	1.15	-
			29	1.33	7.35	-	-
Freon 11	8.0	410	136*	-	-	-	-
			101	1.00	1.40	0.48	-
Hydrogen Chloride	6.8	900	36*	0.34	1.12	-	-
Hydrogen Sulfide	8.8	900	34	0.36	1.36	2.25	-
Methane	10	900	16	0.3	0.08	-	-

TABLE 6 (continued)

COMPOUND	CONCENTR. IN CARRIER GAS	ACCELER. VOLTAGE	MASS NO	IONIZING WAVELENGTH (Å)			
	%		amu	803	950	1048	1216
Methyl Alcohol	4.6	900	32	0.30	1.05	1.10	-
			31	0.50	0.11	1.07	-
Methylene Chloride	8.7	600	84*	0.78	1.45	1.45	-
			49	0.81	1.49	-	-
Nitric Oxide	7.5	900	30	1.00	1.00	1.00	1.00
Nitrogen Dioxide	1.6	900	46	0.38	1.17	0.26	0.03
Propionaldehyde	3.1	850	58	0.76	1.58	1.76	4.18
			29	1.22	0.87	0.07	-
Sulfur Dioxide	12	900	64	0.30	1.84	-	-
Toluene	3.0	500	92	0.175	0.31	0.97	2.9
Vinyl Chloride	9.1	800	62*	1.03	2.63	2.50	2.3
m-Xylene	0.79	500	106	0.45	0.36	3.30	4.60
			91	0.90	0.56	1.59	-
o-Xylene	0.95	500	106	0.29	0.40	2.61	3.36
			91	0.62	0.60	1.28	-
p-Xylene	0.98	500	106	0.18	0.16	3.1	4.50
			91	0.37	0.19	1.58	-

* $^{35}C\ell$ isotope parent peak.

The ratio of light intensities in this expression is simply the ratio of the photomultiplier signals. The response of the sodium salicylate phosphor with which the photomultiplier view plate is coated is proportional to the light intensity. It is also independent of wavelength over a wide range, including the wavelength region employed here (Ref. 10). Thus, the photomultiplier signal is a direct measure of the light intensity. The involved proportionality factor will be derived in a subsequent section.

The influence of the acceleration voltage on the ion collection efficiency, and thus on the sensitivity, had to be determined by auxiliary measurements. Nitric oxide was the sample gas used in this experiment. The results are shown in Figure 7 on an arbitrary scale. Data were obtained on two different days and two ionizing wavelengths, 1216 and 1048Å. It is apparent, that the sensitivity increases considerably with increasing acceleration voltage. Accordingly, the measurements were made with an acceleration supply voltage setting of 900 volts, whenever possible. Then, the correction factor γ_2/γ_1 is unity. In all the cases, corrections were made on the basis of the data in Figure 7.

Table 6 indicates that the relative sensitivites are of the order of unity at the two longest wavelengths, 1216 and 1048Å, and that they decrease at shorter wavelengths. This is due mainly to the increasing fragmentation experienced by the initial photoion.

Absolute sensitivities can be obtained from the data in Table 6, if the absolute sensitivity of nitric oxide is known. Measurements of the sensitivity of nitric oxide were performed from time to time. The results fall into two categories: high values, obtained on the first period, and values lower by about a factor of 5 observed after the instrument was partially disassembled because of the development of an air leak. The averaged results of these two groups of measurements are shown in Table 7. Since the absolute sensitivites are a function of the light intensities, the average photomultiplier readings for which these sensitivities are valid are also given in Table 7. There is no reason to suspect that the sudden drop in sensitivity is due to a change in the gain of the electron multiplier detector, the grating efficiency, the sodium salicylate conversion efficiency, etc. The efficiencies of these components do show a decrease with time, but the change is slow and gradual, never sudden. For example, the electron multiplier gain has been found to decrease gradually over the years, and its supply voltage which initially was set to 2200 volts had to be increased to 3000 volts in the present work to compensate for the decay. The most likely cause for the sudden drop of sensitivity appears to be a loss of ion collection efficiency due to errors in the alignment of the ion source components. Since this factor can be corrected, it appears reasonable to adopt the set of high sensitivity values and to let them represent the practical sensitivity of the instrument. On this basis, the relative sensitivities

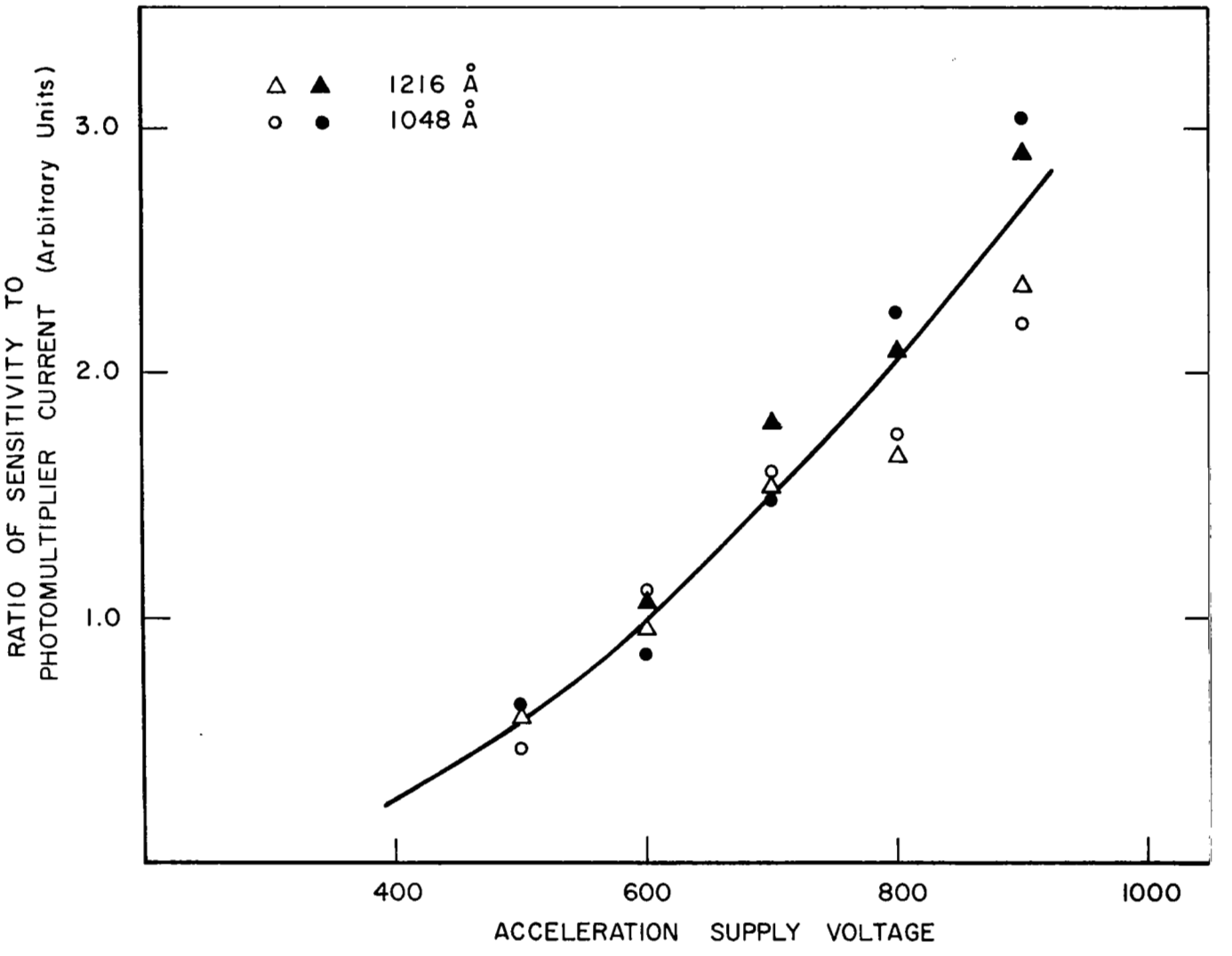

Figure 7. Sensitivity versus acceleration voltage.

TABLE 7

AVERAGE PHOTOMULTIPLIER SIGNALS AND TYPICAL MASS SPECTROMETER SENSITIVITIES FOR NITRIC OXIDE*

WAVELENGTH (Å)		803	950	1048	1216
Photomultiplier signal (10^{-9} amps)		8.7 ± 2.6	5.6 ± 1.4	3.2 ± 0.5	6.7 ± 1.9
Light intensity (10^{8} photons/sec)+		7.0 ± 2.0	4.4 ± 1.0	2.5 ± 0.5	5.4 ± 1.0
Sensitivity‡ (10^{-7} amps/torr)	(a)	3.9 ± 2.0	8.7 ± 2.3	4.2 ± 1.5	2.0 ± 0.7
	(b)	6.6 ± 2.5	1.35 ± 0.3	0.71 ± 0.2	0.40 ± 0.15

* Conditions: Photomultiplier supply voltage 600 volts. Electron-multiplier voltage 3000 volts. Accelerator supply voltage 900 volts. Spark Light source operated with argon at 200 microns pressure, 65 milliamps; dc Light source operated with argon (1048Å), or argon mixed with hydrogen (1216Å) at 800 microns pressure, 280 milliamps.

\+ See Section III.F for a derivation of light intensities.

‡ (a) before and (b) after ion source reassembly required to fix a leak in the system.

in Table 6 can be put on an absolute scale. The resulting sensitivity values are listed in Table 8. Most of the sensitivities derived in this manner lie in the 10^{-7} to 10^{-6} ampere/torr range. Occasionally, sensitivity values lower or higher by a factor of 10 are observed.

D. Problems with NO_2

The behavior of nitrogen dioxide had to be investigated in detail, because at wavelengths above the threshold for NO^+ formation the NO_2 mass spectra showed peaks at m/e = 30 (attributable to NO^+), the intensities of which were comparable to those of NO_2^+ at m/e = 46. Owing to the possibility that nitrogen dioxide was contaminated with NO, a series of experiments were performed designed to determine the origin of the observed NO^+ signal. The results are shown in Table 9.

NO_2 was taken directly from a lecture bottle, added to the evacuated inlet system of the photoionization mass spectrometer, and then admitted to the ion source of the instrument via the sample inlet valve. Source pressures ranged from 0 to 5 microns as indicated by the Hastings thermocouple gauge. As described in Section II. C., the inlet system was provided with a dry ice-acetone cold trap, by means of which NO_2 could be frozen out without affecting NO.

It was first attempted to purify NO_2 by freezing it into the trap, so that any NO impurity could be pumped off. The purified NO_2 indicated a slight but not significant improvement in the observed NO^+/NO_2^+ ions current ratios, as Table 9 testifies. If the dry ice acetone bath was applied to the trap while NO_2 was admitted to the mass spectrometer, both the peaks at m/e = 30 and m/e = 46 vanished simultaneously. Thus, the mass 30 peak did not originate from an NO impurity. Rather, it appeared that NO was produced by a chemical reaction involving NO_2 and parts of the inlet system. Since the brass valve used for regulating the sample flow into the ion source was a likely point of interaction, it was replaced by a stainless steel valve. This measure reduced the NO^+/NO_2^+ ion current ratio measured at 1216Å by a factor of about 4. Further improvement was attained when the apiezon stopcock grease used in the inlet system was replaced by Kel F grease. In each case, it was found that the mass spectrometer signals for NO_2^+ and NO^+ were proportional with pressure up to 5 microns, so that it is unlikely that NO^+ is generated by an ion-molecule reaction of NO_2^+. The data in Table 9 quite clearly imply that the main origin of NO^+ is NO formed by interaction of NO_2 with parts of the inlet system. The absolute sensitivities observed in conjunction with these experiments are also listed in Table 9. These values were corrected by an appropriate factor so that they can be compared directly to those obtained with NO_2 in a carrier gas and listed in Table 8. It appears that the sensitivites observed with pure NO_2 are lower than when mixed into a carrier gas. The reason for this discrepancy

TABLE 8

ABSOLUTE SENSITIVITIES (10^{-7} amps/torr) AT FOUR WAVELENGTHS. CONDITIONS AS GIVEN IN TABLE 7.

COMPOUND	MASS NO amu	IONIZING WAVELENGTH (Å)			
		803	950	1048	1216
Acetone	58	9.8	8.7	5.7	10.8
	43	33.5	8.7	1.3	-
Acetaldehyde	44	17.5	6.3	7.35	-
	29	18.7	1.65	-	-
Allyl Alcohol	58	0.39	0.43	3.15	3.6
	57	1.95	2.18	10.5	-
Ammonia	17	18	5.3	2.31	0.066
Benzene	78	6.6	5.8	25.6	15.6
Butene-1	56	31.6	20	23.4	5.65
cis-Butene-2	56	16.8	16.8	8.4	6.20
	41	23.0	19.0	-	-
trans-Butene-2	56	16.8	16.8	8.8	9.50
	41	25.3	19.0	-	-
n-Butyl Alcohol	74	3.04	2.8	0.55	0.48
	56	10.0	87	6.95	0.34
iso-Butyl Alcohol	74	8.2	3.65	2.18	1.10
	33	25.7	10.3	4.82	-
	43	42.8	12.2	1.38	-
sec-Butyl Alcohol	74	10.5	2.61	0.17	0.42
	44	38.5	46.0	1.85	1.50
	45	350	87	4.20	0.074
tert-Butyl Alcohol	74	-	-	-	-
	59	10.9	47	13.9	4.20
Carbon Disulfide	76	156	71	130	9.6
1,4 Dioxane	88	1.05	0.84	3.02	3.04
	28	3.55	0.87	-	-
Ethyl Acetate	88	0.34	0.55	1.72	0.88
	43	3.78	1.02	0.07	-
Ethylene Dichloride	98	5.45	1.74	0.97	-
	62	7.00	2.35	1.09	-
	27	8.60	0.11	-	-
Formaldehyde	30	42.8	26.1	4.03	-
	29	52.0	10.0	-	-
Freon 11	136	-	-	-	-
	101	39	12.2	2.0	-
Hydrogen Chloride	36	13.3	9.7	-	-
Hydrogen Sulfide	34	14.0	11.8	9.5	-
Methane	16	11.7	0.7	-	-

TABLE 8 (continued)

COMPOUND	MASS NO amu	IONIZING WAVELENGTH (Å)			
		803	950	1048	1216
Methyl Alcohol	32	11.7	9.1	4.62	-
	31	19.5	0.95	4.5	-
Methylene Chloride	84	30.4	12.6	6.1	-
	49	31.5	12.9	-	-
Nitric Oxide	30	39.0	8.7	4.2	2.0
Nitrogen Dioxide	46	14.8	10.2	1.08	0.06
Propionaldehyde	58	29.6	13.7	7.4	8.36
	29	47.5	7.6	0.29	-
Sulfur Dioxide	64	11.7	16.0	-	-
Toluene	92	68.2	2.70	4.1	5.8
	91	12.8	2.08	-	-
Vinyl Chloride	62	40	22.9	10.5	4.6
m-Xylene	106	17.6	3.13	13.8	9.2
	91	35.1	4.87	6.7	-
o-Xylene	106	11.3	3.48	11.0	6.72
	91	24.2	5.22	5.4	-
p-Xylene	106	7.0	1.39	13.0	9.0
	91	14.4	1.65	6.6	-

TABLE 9

NO^+/NO_2^+ ION CURRENT RATIOS AND NO_2 SENSITIVITIES OBSERVED FOR DIFFERENT EXPERIMENTAL CONDITIONS

CONDITIONS	WAVELENGTH (Å)	$i(NO^+)/i(NO_2^+)$	SENSITIVITY NO_2 (amp/torr)
Unpurified NO_2	1216	3.95	0.97×10^{-9}
Purified NO_2 with brass valve	1216	2.15	1.15×10^{-9}
Purified NO_2 with stainless valve	1216	0.57	1.00×10^{-9}
Purified NO_2 with stainless steel valve and Kel-F stop-cock grease	1216	0.15	1.14×10^{-9}
	1048	0.02	1.84×10^{-8}

probably is the different response of the thermocouple gauge in the two cases. It is of interest to note that the sensitivity for NO_2 at m/e = 46 is not affected by the generation of NO from NO_2 in the inlet system, indicating that the NO impurity is comparatively small. Indeed, from the relative sensitivities for NO and NO_2, the amount of NO impurity present is estimated to range from 0.5 to 10 percent. The considerable influence of the NO impurity on the mass spectrum is due to the relatively small sensitivity of NO_2 at the ionizing wavelength 1216Å. The sensitivity for NO_2 at 1048Å is about ten times that at 1216Å so that the effect of any NO impurity is lessened. At 950 and 803Å, NO^+ is a fragment resulting from NO_2 ionization. In this wavelength range the present data are in reasonable agreement with those obtained by Dibeler, et al. (Ref. 11) in an independent study.

E. Detection Limits

As a counterpart to the instrumental sensitivity for a given substance, it is desirable to know the lowest limit of the sample concentration that one can detect. Apart from the sensitivity, the detection limit depends on two factors: the background noise level of the electrometer output, and the optimum sample pressure in the ion source. Both factors may vary considerably with experimental conditions, so that absolute detection limits are subject to even greater uncertainty than absolute sensitivities.

High pressures of sample in the ion source obviously are favorable for achieving low detection limits, but as discussed previously, the useful pressure range is bounded for most applications by nonlinearities resulting from ion-neutral reactions, saturation effects, etc. However, if the sample is contained in a carrier gas which does not ionize at the employed wavelength, and if the sample concentration is sufficiently small, the upper limit pressure in the ion chamber is determined only by the capacity of the pumps. In this case, the pressure may be as high as 100 microns. Air qualifies as a carrier gas at the wavelengths 1216 and 1048Å; nitrogen and helium at all four wavelengths employed in the present study.

The background noise of the electrometer depends critically on the quality of the cable and the connections coupling the electrometer input to the electron multiplier output. In addition, the noise level is given by the electron multiplier dark current, high frequency noise from the spark source and other external sources, and the time constant of the electrometer output. With the time constant set to 1 second (full damping) and the electron multiplier supply voltage set to 3000 volts, the electrometer background noise level is approximately 5×10^{-15} amperes. High humidity, inadequate shielding, worn spark source points, etc. may increase the noise level.

For the calculation of detection limits, it may be assumed that a signal can be observed if it equals or exceeds the noise level. Thus the detection limit is defined as

$$L(\text{ppm}) = 10^6 \frac{p}{p_t} = \frac{10^6 N}{S p_t}$$

where p is the partial pressure of a substance in the ion source, p_t the total ion source pressure, N the noise level in amperes, and, S the sensitivity of the instrument for the substance under consideration. The values adopted for the derivation of detection limits are $N = 5 \times 10^{-15}$ amperes, $p_t = 10^{-3}$ torr, with the sensitivities given in Table 8. The calculated detection limits are summarized in Table 10. From the remarks above, it is evident that noise levels higher than 5×10^{-15} amperes may be encountered under adverse conditions, but the choice of ion source pressure deliberately is conservative, so that the ratio of N/p_t may be optimized. Hence, the detection limits given in Table 10 provide a realistic assessment of the detection capabilities of the photoionization technique. In most cases, the detection limits lie in the 5 to 50 ppm concentration range.

F. Efficiency of Instrumentation

In this section, a set of experiments will be described by which the efficiency of the instrumentation can be determined. For this purpose, one requires measurements of, (a) the light flux through the ion source and the associated ion production, (b) the ion current entering the magnetic analyzer, and (c) the gain provided by the electron multiplier.

(a) To determine the light flux and ion yield, the ion source was used as an ionization chamber. The ion draw-out electrode of the ion source was connected to the Keithley electrometer. The body of the ion source and the repeller were jointly connected to the positive lead of a 22-volt battery. The other lead was grounded. The battery supplied the potential necessary to drive essentially all ions formed within the ion source to the draw-out plate which thus acted as the ion collecter. No other fields were employed. The dc source operated with hydrogen was used in these experiments and the monochromator was initially set to 1216Å. Nitric oxide was employed as the ionizable gas, because it had served as the reference gas throughout the course of the present work and its ionization cross section at 1216Å is well known. The ion current observed in this manner is

$$j_i = e\, \sigma_i(\text{NO})\, n\, L\, I_o$$

where $e = 1.6 \times 10^{-19}$ Coulombs, $\sigma_i(\text{NO}) = 1.95 \times 10^{-18}$ cm^2 is the photoionization cross section of NO (Ref. 12), n the NO gas density, L = 1.28 cm the length of the ionization region and I_o the light intensity in photons/sec.

TABLE 10

DETECTION LIMITS IN PARTS PER MILLION DERIVED FROM THE SENSITIVITIES GIVEN IN TABLE 8

COMPOUND	MASS NO		IONIZING WAVELENGTH (Å)			
	amu		803	950	1048	1216
Acetone	58		5	6	9	5
	43		2	6	38	-
Acetaldehyde	44		3	8	7	-
	29		3	30	-	-
Allyl Alcohol	58		128	110	16	14
	57		26	24	5	-
Ammonia	17		28	10	22	750
Benzene	78		8	9	2	3
Butene-1	56		2	3	2	9
cis-Butene-2	56		3	3	6	8
	41		2	3	-	-
trans-Butene-2	56		3	3	6	6
	41		2	3	-	-
n-Butyl Alcohol	74		17	18	92	105
	56		5	<1	8	148
iso-Butyl Alcohol	74		6	14	23	45
	33		2	5	10	-
	43		0.2	4	36	-
sec-Butyl Alcohol	74		5	19	290	120
	44		2	1	27	33
	45		<1	<1	12	670
tert-Butyl Alcohol	74		-	-	-	-
	59		5	1	4	12
Carbon Disulfide	76		<1	<1	<1	5
1,4 Dioxane	88	*	48	59	17	17
	28		14	55	-	-
Ethyl Acetate	88	*	147	91	29	570
	43		13	49	72	-
Ethylene Dichloride	98	*	9	29	52	-
	62		7	21	46	-
	27		6	455	-	-
Formaldehyde	30		1	2	11	-
	29		1	5	-	-
Freon 11	136	*	-	-	-	-
	101		2	4	25	-
Hydrogen Chloride	36		4	6	-	-
Hydrogen Sulfide	34		4	4	6	-
Methane	16		4	71	-	-
Methyl Alcohol	32		4	6	11	-
	31		3	6	11	-

TABLE 10 (continued)

COMPOUND	MASS NO		IONIZING WAVELENGTH (Å)			
	amu		803	950	1048	1216
Nitric Oxide	30		2	6	12	25
Nitrogen Dioxide	46		4	5	46	835
Propionaldehyde	58		2	4	7	6
	29		1	7	172	-
Sulfur Dioxide	64		4	3	-	-
Toluene	92	*	<1	19	12	9
	91		4	24	-	-
Vinyl Chloride	62		2	3	5	11
m-Xylene	106	*	3	16	4	6
	91		2	10	8	-
o-Xylene	106	*	5	15	5	8
	91		2	10	10	-
p-Xylene	106	*	7	4	4	6
	91		4	30	8	-

* All values are derived for an ion accelerating voltage of 900 volts. The corresponding mass range is 0 to 75 amu. The asteric indicates those substances, for which the parent peak lies outside this range, and the mass scale has to be expanded by lowering the acceleration voltage. Then, the detection limits are higher by a factor of about two.

A flow of nitric oxide was established which provided a pressure of 10 microns of nitric oxide in the ion chamber, i.e. $n = 3.3 \times 10^{14}$ molecules/cm^3. The ion current measured after exposure of the ion source to 1216Å light was 1×10^{-13} amperes, the associated photomultiplier signal was 0.95×10^{-8} amperes with the photomultiplier supply voltage set to 600 volts. From the ion current generated, one calculated that the light intensity for this experiment is 7.6×10^8 photons/sec. The relation between the photomultiplier output signal I (PM) and the light intensity then is $I_o = 8 \times 10^{16}$ I (PM) for the employed operating conditions. This relationship has been used to derive the average light intensities indicated in Table 7 for the four wavelengths employed.

(b) To determine the efficiency of ion collection, the electrometer was first connected to the auxiliary ion collector provided in the rear of the magnetic analyzer. For this measurement, the ion current generated by the 1216Å Lyman-alpha line was insufficient, and the monochromator was set to the central image, so that the undispersed light emitted from the dc source was transmitted. The acceleration potential was set to 900 volts, no magnetic field was applied, and the registered ion beam was focused to optimum intensity. The current then registered was 2.8×10^{-12} amperes. The ion current observed with the electrometer connected to the ion source draw-out plate was 1.5×10^{-11} amperes under equivalent conditions (but with the acceleration voltage switched off), so that in this particular experiment only 18 percent of the ions formed in the source were collected and entered the mass analyzer. It should be noted, however, that these experiments were performed toward the end of the series of measurements. Since a sudden drop of mass spectrometer sensitivity had occurred at one point during the investigation, and since the sensitivity loss factor was approximately five, it appears that a reasonably complete ion collection efficiency can be achieved.

(c) The electron multiplier gain was measured in conjunction with the above experiment. For this purpose, the electron multiplier was supplied with a total potential of 3000 volts a magnetic field was established and the magnet current was adjusted to transmit the NO^+ ion. The output current at m/e = 30 was 4.1×10^{-7} amperes. By comparison with the ion current entering the mass analyzer, 2.8×10^{-12} amperes, the gain is determined as G = 147000. This factor includes possible losses of ions at the mass analyzer exit slit. For a check on the collection efficiency, the monochromator grating was turned back to the position of the 1216Å Lyman-alpha line. The measured output current in this case was 2.7×10^{-9} amperes at m/e = 30, from which one infers an ion current of 1.85×10^{-17} amperes entering the mass analyzer. Since the ion production at the Lyman-alpha line had been found above to yield an ion current of 1×10^{-13} amperes, an ion collection efficiency of 18 percent is again indicated.

G. Mixtures

The photoionization mass spectrometer was further tested with the investigation of five gas mixtures containing at least three components. The composition of the investigated mixtures is given in Table 11. Also shown in the table are the ionization threshold wavelengths for the individual components. The first three mixtures contain vapors which are miscible in liquid form. These mixtures were initially prepared by mixing the individual components in the desired ratio and injecting a portion of the mixture into a 12-liter flask previously evacuated and filled with helium. Equilibration of the mixture in the flask was extremely slow and still incomplete after 48 hours, so that injection procedure was modified in that each component was injected separately into the evacuated sample flask and helium was added subsequently.

The ionizing wavelengths used in these experiments were 1216 and 1048Å. The results obtained are summarized in Tables 12 through 16. For each mixture, the tables give the sensitivity for the occurring ions due to the individual components, their partial pressures in the ion source calculated from the total pressure and the prepared concentrations, the calculated sum of the signals at each mass number, and the observed signals. Generally, there is good agreement between observed and calculated ion signals, although in a few cases the agreement is valid only within a factor of 2.

The individual mixtures may now be discussed:

Mixture No. 1 comprises components which exhibit only their parent ion peaks if the ionizing wavelength is 1216Å, so that the mass spectrum consist of only four non-interfering peaks. Accordingly, the analysis of such a mixture is made convenient.

Mixture No. 2 contained the four structural isomers of the butyl alcohols all of which have different fragmentation patterns and sensitivities throughout the investigated wavelength range (> 800Å). The wavelength 1048Å was selected for the present purpose, because at this wavelength the mass spectra of the individual components are still simple but are also sufficiently differentiated for a quantitative analysis. In this mixture, several mass peaks are due predominantly to one component. Thus, m/e = 56 derives essentially from n-butyl alcohol, m/e = 74 and m/e = 33 essentially from iso-butyl alcohol, m/e = 45 and m/e = 59 essentially from tert-butyl alcohol. The analysis of mixtures containing these compounds is thereby facilitated.

Mixture No. 3 consists of three functional isomers which also show different fragmentation patterns and sensitivities as a function of wavelength. Two ionizing wavelengths were used in the investigation of this mixture: 1216 and 1048Å. The former gives mainly the parent peaks, so that an effective discrimination is not provided, whereas the latter generates isolated features in the mass spectral patterns of allyl alcohol and acetone.

TABLE 11

COMPOSITION OF MIXTURES

IDENTIFICATION NO.	COMPOUNDS	CONCENTRATION %	THRESHOLD WAVELENGTH (Å)
#1	p-Xylene	0.30	1462
	Toluene	0.70	1405
	1,4 Dioxane	0.44	1358
	Benzene	0.84	1341
	Helium	Balance	502
#2	n-Butyl Alcohol	0.20	1246
	iso-Butyl Alcohol	0.40	1252
	sec-Butyl Alcohol	0.81	1259
	tert-Butyl Alcohol	0.79	1244
	Helium	Balance	502
#3	Allyl Alcohol	1.10	1279
	Proprionaldehyde	1.04	1242
	Acetone	2.50	1279
	Helium	Balance	502
#4	Ethylene Dichloride	1.30	1114
	Methylene Dichloride	1.25	1092
	Benzene	0.91	1341
	Carbon Disulfide	1.32	1230
	Vinyl Chloride	1.45	1239
	Acetone	1.36	1279
	Hydrogen Sulfide	2.5	1185
	Nitric Oxide	1.85	1340
	Air	Balance	1027
#5	Ethylene Dichloride	1.30	1114
	Methylene Dichloride	1.25	1092
	Benzene	0.91	1341
	Carbon Disulfide	1.32	1230
	Vinyl Chloride	1.90	1239
	Acetone	1.36	1279
	Hydrogen Sulfide	1.85	1185
	Air	Balance	1027

TABLE 12

INDIVIDUAL COMPONENT PEAK SENSITIVITIES s, ION SOURCE PARTIAL PRESSURE p, AND CORRESPONDING SIGNAL CURRENTS FOR MIXTURE NO. 1, IONIZING WAVELENGTH 1216Å

m/e	Individual Component Peak Sensitivities (s), amps/torr				Sum of ion currents $\Sigma(s \times p)$, amps	
	p-xylene	toluene	p-dioxane	benzene	Calculated	Observed
106	1.43×10^{-7}				3.43×10^{-13}	1.50×10^{-13}
92		1.32×10^{-7}			7.38×10^{-13}	6.60×10^{-13}
88			4.53×10^{-8}		1.59×10^{-13}	1.50×10^{-13}
78				9.05×10^{-8}	6.07×10^{-13}	7.80×10^{-13}
p(torr)	2.4×10^{-6}	5.6×10^{-6}	3.5×10^{-6}	6.7×10^{-6}		

TABLE 13

INDIVIDUAL COMPONENT PEAK SENSITIVITIES s, ION SOURCE PARTIAL PRESSURE p, AND CORRESPONDING SIGNAL CURRENTS FOR MIXTURE NO. 2, IONIZING WAVELENGTH 1048Å

m/e	Individual Component Peak Sensitivities (s), amps/torr				Sum of ion currents $\Sigma(s \times p)$, amps	
	n-butyl	iso-butyl	sec-butyl	tert-butyl	Calculated	Observed
74	3.28×10^{-9}	1.41×10^{-8}	1.12×10^{-9}	-	1.01×10^{-13}	1.26×10^{-13}
59	-	-	1.19×10^{-8}	1.09×10^{-7}	1.34×10^{-12}	1.33×10^{-12}
57	2.27×10^{-9}	3.90×10^{-9}	6.90×10^{-10}	3.80×10^{-9}	7.81×10^{-14}	7.20×10^{-14}
56	5.55×10^{-8}	4.70×10^{-9}	6.90×10^{-10}	-	1.90×10^{-13}	2.10×10^{-13}
45	-	-	3.23×10^{-8}	-	3.66×10^{-13}	8.55×10^{-13}
44	-	1.20×10^{-9}	1.20×10^{-8}	-	1.43×10^{-13}	3.06×10^{-13}
43	2.27×10^{-9}	9.40×10^{-9}	-	-	5.90×10^{-14}	6.90×10^{-14}
33	2.27×10^{-9}	3.10×10^{-8}	-	-	1.80×10^{-13}	2.52×10^{-13}
p(torr)	2.8×10^{-6}	5.6×10^{-6}	1.13×10^{-5}	1.11×10^{-5}		

TABLE 14

INDIVIDUAL COMPONENT PEAK SENSITIVITIES s, ION SOURCE PARTIAL PRESSURE p, AND CORRESPONDING SIGNAL CURRENTS FOR MIXTURE NO. 3, IONIZING WAVELENGTH 1216Å

m/e	Individual Component Peak Sensitivities (s), amps/torr			Sum of ion currents $\Sigma(s \times p)$, amps	
	allyl alcohol	propionaldehyde	acetone	Calculated	Observed
59	5.68×10^{-9}	2.89×10^{-8}	2.00×10^{-8}	5.62×10^{-13}	9.00×10^{-13}
58	1.50×10^{-7}	5.71×10^{-7}	5.40×10^{-7}	1.37×10^{-11}	1.29×10^{-11}
57	2.39×10^{-8}	-	-	1.71×10^{-13}	1.80×10^{-13}
p(torr)	7.15×10^{-6}	6.76×10^{-6}	1.63×10^{-5}		

MIXTURE NO. 3, IONIZING WAVELENGTH 1048Å

m/e	Individual Component Peak Sensitivities (s), amps/torr			Sum of ion currents $\Sigma(s \times p)$, amps	
	allyl alcohol	propionaldehyde	acetone	Calculated	Observed
59	4.85×10^{-9}	2.31×10^{-8}	6.00×10^{-9}	2.66×10^{-13}	3.30×10^{-13}
58	7.57×10^{-8}	2.77×10^{-7}	1.43×10^{-7}	4.35×10^{-12}	3.97×10^{-12}

TABLE 14 (continued)

m/e	Individual Component Peak Sensitivities (s), amps/torr			Sum of ion currents $\Sigma(s \times p)$, amps	
	allyl alcohol	propionaldehyde	acetone	Calculated	Observed
57	2.55×10^{-7}	4.21×10^{-8}	8.00×10^{-9}	2.06×10^{-12}	1.40×10^{-12}
43	-	-	4.80×10^{-8}	7.20×10^{-13}	7.20×10^{-13}
40	1.00×10^{-8}	-	-	6.60×10^{-14}	5.40×10^{-14}
30	4.34×10^{-8}	-	-	2.86×10^{-13}	2.61×10^{-13}
29	6.97×10^{-9}	1.56×10^{-8}	-	1.43×10^{-13}	4.50×10^{-14}
28	6.06×10^{-9}	-	-	4.01×10^{-14}	3.60×10^{-14}
p(torr)	6.6×10^{-6}	6.24×10^{-6}	1.5×10^{-5}		

TABLE 15

INDIVIDUAL COMPONENT PEAK SENSITIVITIES, AND CORRESPONDING SIGNAL CURRENTS FOR MIXTURE NO. 4 AND NO. 5, IONIZING WAVELENGTH 1216Å

m/e	Individual Component Peak Sensitivities (s), amps/torr					Sum of ion currents Σ(s x p), amps			
						Mixture #4		Mixture #5	
	C_6H_6	CS_2	Vinyl Chloride	Acetone	NO	Calculated	Observed	Calculated	Observed
78	0.97^{-7}	-	-	-	-	1.95^{-12}	1.8^{-12}	2.21^{-12}	2.0^{-12}
76	-	2.4^{-7}	-	-	-	7.00^{-12}	0.9^{-12}	8.00^{-12}	7.5^{-12}
64	-	-	2.15^{-8}	-	-	6.90^{-13}	5.3^{-13}	1.03^{-12}	1.2^{-12}
63	-	-	2.15^{-9}	-	-	6.90^{-14}	5.5^{-14}	1.03^{-13}	1.1^{-13}
62	-	-	7.2^{-8}	-	-	2.30^{-12}	2.1^{-12}	3.42^{-12}	3.5^{-12}
58	-	-	-	1.56^{-7}	-	4.70^{-13}	4.0^{-13}	5.33^{-13}	5.0^{-13}
30	-	-	-	-	1.56^{-7}	5.10^{-13}	*	-	-

*Not detected

p = partial pressure of component in the ion source

Total ion source pressure
was 2.2μ for Mixture #4

was 2.5μ for Mixture #5

Superscripts indicate powers of ten; e.g. $0.97^{-7} = 0.97 \times 10^{-7}$.

TABLE 16

INDIVIDUAL COMPONENT PEAK SENSITIVITIES, AND CORRESPONDING SIGNAL CURRENTS FOR MIXTURE NO. 4 AND NO. 5, IONIZING WAVELENGTH 1048Å

m/e	Individual Component Peak Sensitivities (s), amp/torr								Sum of ion currents, Σ(s x p), amps			
									Mixture #4		Mixture #5	
	Eth $C\ell_2$	Meth $C\ell_2$	C_6H_6	CS_2	Vinyl $C\ell$	Acetone	H_2S	NO	Calculated	Observed	Calculated	Observed
102	1.5^{-10}	-	-	-	-	-	-	-	4.3^{-15}	8^{-15}	4.9^{-15}	6.5^{-15}
100	1.10^{-9}	-	-	-	-	-	-	-	3.15^{-14}	6^{-14}	3.6^{-14}	4.5^{-14}
98	1.48^{-9}	-	-	-	-	-	-	-	4.22^{-14}	10^{-14}	4.8^{-14}	6.0^{-14}
88	-	1.95^{-9}	-	-	-	-	-	-	5.35^{-14}	4.5^{-14}	6.1^{-14}	5.5^{-14}
86	-	1.15^{-8}	-	-	-	-	-	-	3.17^{-13}	2.9^{-13}	3.6^{-13}	3.2^{-13}
84	-	1.78^{-8}	-	-	-	-	-	-	4.9^{-13}	3.9^{-13}	5.6^{-13}	5.1^{-13}
78	-	-	5.60^{-8}	-	-	-	-	-	1.13^{-12}	1.15^{-13}	1.28^{-12}	1.3^{-12}
76	-	-	-	1.20^{-6}	-	-	-	-	3.5^{-11}	0.5^{-11}	4.0^{-11}	3.5^{-11}
64	8.0^{-10}	-	-	-	1.54^{-8}	-	-	-	5.1^{-13}	4.5^{-13}	7.5^{-13}	8.0^{-13}
63	2.68^{-10}	-	-	-	1.50^{-9}	-	-	-	5.5^{-14}	7.5^{-14}	7.8^{-14}	6.0^{-14}
62	1.90^{-9}	-	-	-	4.50^{-8}	-	-	-	1.5^{-12}	1.35^{-12}	2.7^{-12}	2.8^{-12}
58	-	-	-	-	-	2.70^{-8}	-	-	8.1^{-13}	7.0^{-13}	9.2^{-13}	10.5^{-13}
43	-	-	-	-	-	6.30^{-9}	-	-	1.9^{-13}	1.5^{-13}	2.15^{-13}	2.4^{-13}
34	-	-	-	-	-	-	1.74^{-8}	-	9.6^{-13}	*	8.1^{-13}	8.5^{-13}
30	-	-	-	-	-	-	-	6.20^{-9}	2.5^{-13}	*	-	-

*Not detected, p = partial pressure of component in the ion source.

Total ion source pressure
was 2.2μ for Mixture #4

was 2.5μ for Mixture #5

Superscripts indicate powers of ten; e.g. $1.5^{-10} = 1.5 \times 10^{-10}$.

Mixtures No. 4 and 5 are almost identical except that mixture No. 4 contains nitric oxide whereas mixture No. 5 does not. These mixtures contain air as a carrier gas, which reacts with NO to form NO_2 so that their comparison provided a test for the reactivity of NO-NO_2 with other components in the mixtures. At the end of the equilibration period, mixture No. 4 was found to have lost its brownish color due to NO_2. In addition, some crystalline products appeared to have deposited on the walls. Evidently, a reaction had occurred between NO_2 and some of the other components. In mixture No. 5, no reaction was apparent. The occurrence of a reaction is demonstrated more quantitatively by the results shown in Tables 15 and 16. In mixture No. 4, nitric oxide and hydrogen sulfide could not be recovered. In addition, a loss occurred for carbon disulfide, whereas the other components were essentially unaffected. In the mixture not containing NO, the hydrogen sulfide and the carbon disulfide could be completely recovered. It is possible that the reaction does not directly involve nitrogen dioxide or nitric oxide on one hand, and hydrogen sulfide and carbon disulfide on the other, but that the reaction is catalyzed by moisture introduced with the air. No attempts have been made to investigate this point.

Again it can be noted that the use of two ionizing wavelengths, 1216 and 1048Å, allows a complete separation of the mass spectrometer signals at the various mass numbers.

From the data present here, it is concluded that the majority of the observed peak heights are within 20 percent of the calculated ones. Because of uncertainties in the sample preparations, sensitivities were redetermined with the first three mixtures on the same day, and these were used in the tables. Nevertheless, in some cases the observed signal strength differed from the calculated one by a factor of two. Thus, it appears that the errors are due mainly to the uncertainties in preparing the samples, individually and in mixtures.

IV. CONCLUSIONS

A. Application to Trace Gas Analysis

The results presented in the preceding sections indicate quite generally the excellent performance of the photoionization mass spectrometer when applied to gas analysis. The derived sensitivities and detection limits are in accord with the expectation that for ion source pressures of about 1 micron, gas concentrations of the order of 10 ppm can be detected by the regular scanning of the mass spectrum. For many organic vapors the analytical capability is even better, providing detection limits around 1 ppm. However, although this capability meets the demands of many analytical applications, it still is insufficient for the direct analysis of trace gas contaminants which requires a detection limit of equal or less than 0.1 ppm. The question, therefore, is whether the photoionization mass spectrometer technique provides room for further development. This aspect will now be discussed. In Section III, it was shown that the detection limit depends on the three factors: sensitivity, ion source pressure, and background noise level. Any improvement should then be concerned with these quantities.

The sensitivity increases with the gain of the electron multiplier and the light intensity. The gain of the electron multiplier can be increased by perhaps a factor of 10, but with the present mode of direct current readout this measure would not really result in an improvement because the dark current and thus the noise level would also increase. An improvement in signal to noise ratio must be attained by other methods which will be discussed further below. The light intensity can be increased if the monochromator is operated with wider slits and correspondingly lower spectral resolution. It is estimated that a gain by a factor of 5 in light intensity can be achieved in this manner. The optical resolution will be about 50Å full width, compared with 7Å under present conditions. Adverse effects by the poorer spectral resolution are not anticipated. In addition to working with wider optical slits, one can improve on the transmission of the monochromator by reducing the astigmatism involved with spherical gratings. Use of a toroidal grating instead of the common concave grating will provide nearly stigmatic focusing. The resulting gain in light transmission is about a factor of 5, as Schönheit (Ref. 13) has shown. Together with the increased slit width, the gain factor of light intensity achieved in this manner will be about 20. Toroidal gratings are much more difficult to manufacture than the simpler spherical reflection gratings and the associated cost is correspondingly greater.

The ion source pressure chosen in deriving the detection limits shown in Table 10 was 1 micron. In discussing detection limits, it has been noted that higher ion source pressures can be utilized for the analysis of trace gases, so long as ionization of the principal gaseous component does not cause any secondary interactions. While this possibility has not

been investigated in the present study, it appears that secondary ion interaction is essentially negligible at pressures up to 10 microns in most cases. Accordingly, it will be possible to decrease the detection limit by a factor of 10, if an ion source pressure of 10 microns is used. Together with the above indicated increase in light intensity, the capability of the photoionization mass spectrometer will be improved by a factor of 200, so that the detection limit is lowered to equal or less than 0.1 ppm. It should be noted that such an improvement is achieved without the use of preconcentration procedures.

Additional improvements are feasible, if the signal to noise ratio of the electron multiplier output signal can be improved. One technique described previously, makes use of synchronous detection in conjunction with the spark light source. Gating the electron multiplier output to transmit current only during the arrival of the ion pulse but not during the off-periods will increase the signal-to-noise ratio by a factor of 1000. This technique would significantly reduce the noise associated with the spark light source, but would not be applicable with the dc source. In that case, pulse counting techniques may provide some reduction in the noise level.

In summary, the discussion given here indicates that further instrumental improvements are available to enable the application of photoionization mass spectrometry to trace gas analysis.

B. Application to the Analysis of Spacecraft Cabin Atmospheres

It has been suggested and discussed previously (Ref. 2) that photoionization mass spectrometry might serve as a suitable technique for monitoring the constituents of cabin atmospheres during long range space flight. This application is made attractive by the natural availability of solar uv radiation as the photoionizing agent, so that the power requirements for ionization are minimized. To evaluate this concept the following considerations are pertinent.

The ion detector would be an electron multiplier operated in the counting mode to achieve a minimum noise level. If an accuracy of 10 percent is desired, the minimum number of counts required to obtain this accuracy is 100 counts. If further the efficiency of the detector is such that every ion generates one pulse, and the counting time for each significant ion is 100 seconds, the minimum ion flux required as 1 ion/sec. The background would be less than one-tenth of that value.

The mass analyzer can be of light weight with a minimum of power consumption. Quadrupole or monopole analyzers would provide favorable ion transmission coefficients. A transmission coefficient of 33 percent probably is feasible. Hence, the minimum number of ions to be generated and directed into the analyzer is 3 ions/sec.

Table 17 gives a compilation of solar flux data for the 796 to 1325Å wavelength region. This is the wavelength range which in the present study has been found optimally suited for photoionization mass spectrometry. In the region 800 to 890Å, which ionizes CO but not nitrogen, the solar flux is 8.7×10^9 photons/cm^2 sec at a distance of 1 astronomical unit. The total usable solar ionizing radiation in the region 800 to 1220Å is 3.35×10^{11} photons/cm^2 sec, of which 2.7×10^{11} resides in the hydrogen Lyman-alpha line. While the longer wavelengths may be useful for the ionization of many organic trace molecules, not all the gaseous components will be ionized by it. It is useful, therefore, to consider three values: 8.7×10^9 photons/cm^2 sec for CO, 2.6×10^{10} photons/cm^2 sec for all molecules having an ionization potential greater than 12 eV and 3.3×10^{11} photons/cm^2 sec for molecules with lower ionization potentials.

The ion source can be assumed to consist of a box with apertures for the entrance of radiation and withdrawal of ions. The present study has shown that with ion source dimensions of the order of 1 cm a reasonably complete collection and withdrawal of ions formed inside the source can be achieved through the application of appropriate electric fields. A reasonable size of the radiation entrance aperture is 0.6 cm diameter corresponding to an area of 0.28 cm^2. The solar flux entering the source is, accordingly, 2.4×10^9 photons/sec for the wavelength region 800 to 890Å, and 7.3×10^9 and 9.3×10^{10} photons/sec, respectively, for the other two wavelength regions cited above. Comparison with light intensities and NO sensitivities given in Table 7 indicates, that for nitric oxide the ion currents generated are 2, 6, and 80 ions/sec respectively, if the total ion source pressure is 10 microns and the concentration of NO is 1 ppm. Since Table 6 indicates that the sensitivities for most substances are comparable with those for NO, similar ion production rates are expected for the other substances. If the transmission of the mass analyzer is 33 percent and a nearly complete collection of photoions is realized, the number of ions arriving at the electron multiplier and being counted in a 100-sec time interval is 66,200, and 2,700, respectively, for the wavelength regions indicated above. The corresponding lower limit concentrations which can be measured with 10-percent accuracy are 1.5, 0.5 and 0.035 ppm.

For higher sensitivities, the light gathering power must be increased and a focusing system must be used. Therefore, consider a telescope system to image the sun onto the ion source aperture. The angular diameter of the sun is $\alpha = 0.5$ degrees $\approx 1/120$ radian. The focal length of the telescope required for the re-imaging process is $f = D/\alpha$ where $D = 0.6$ cm is the diameter of the ion source aperture. Then $f = 0.6 \times 120 = 72$ cm. The maximum collection aperture that can be accommodated by the system is determined by the geometry of the ion source. This quantity may be estimated by the expression $A = f\theta$, where θ is the maximum divergence angle permitted by the size of the ion source. It can be assumed that $\theta = 0.5$ radian (f/2 arrangement) so that $A = 36$ cm. The area of a mirror of this size is approximately 1×10^3 cm^2. The increase of light gathering

TABLE 17

INTENSITIES IN SOLAR XUV-SPECTRUM
AT A DISTANCE OF 1 A.U. (AFTER HINTEREGGER)

WAVELENGTH OR RANGE (Å)	IDENTIFICATION	INTENSITIES 10^9 photons/cm^2 sec
1325-1275		11.8
1275-1220		26
1215.7	H Ly-α	270
1206.5	SiIII	4.3
1220-1200	excl. H Ly-α, SiIII	7.4
1200-1180		5.5
1175.7	CIII	2.5
1180-1130	excluding CIII	5.8
1130-1090		4.4
1085.7	NII	0.48
1090-1040	excluding NII	4.2
1037.6	O VI	1.33
1031.9	O VI	1.89
1040-1027	excluding O VI	0.69
1325-1027	total	350
1025.7	H Ly-β	2.3
991.5	NIII	0.33
1027- 990	excl. H Ly-β, NIII	2.4
977.0	CIII	4.0
972.5	H Ly-γ	0.55
990- 950	excl. CIII, H Ly-γ	0.97
949.7	H Ly-δ	0.25
937.8	H Ly-ϵ	0.17
950- 920	excl. H Ly-δ, ϵ	1.07
920- 911		1.25
1027- 911	total	13.4
911- 890	H Ly-continuum	4.0
890- 860	H Ly-continuum	4.2
860- 840	H Ly-continuum	2.0
835- 832	OII, III	0.54
840- 810	excluding OII, III	2.0
810- 796		0.7
911- 796	total	13.4

power over that of the simple 0.6 cm diameter aperture is 3600, but only a portion of it is usable because reflectivities of mirrors in the vacuum ultraviolet region are poor. Optimum reflectivities are achieved by coating the mirror with a 100Å layer of platinum. This results in a reflection of about 15 percent of the incident light. Thus, the light gathering power will be greater by a factor of only 400 to 500. Nevertheless, this arrangement will lead to a photon flux of 1×10^{12} photons/sec for the 800 to 890Å wavelength region, 3×10^{13} photons/sec for the 800 to 1220Å wavelength region. The corresponding limiting concentrations which can be measured with 10-percent accuracy are 4×10^{-3}, 1.2×10^{-3} and 1×10^{-4} ppm, respectively.

Since the above considerations do not include the use of a monochromator, the wavelength regions involved have to be isolated by filters. Specifically, the wavelength region below 800Å has to be completely blocked, so that CO can be detected at m/e = 28 without the interference of nitrogen. Some suitable filters exist. For example, the region below 1000Å can be excluded by a LiF filter. There are also filters available for blocking the wavelength region below 800Å, and these have been discussed previously (Ref. 3, 5). Nevertheless, the production of suitable filters constitutes an important technological problem in the exploitation of this system.

Other problem areas which should be given due consideration in a detailed systems study are: depletion of cabin atmosphere by gas flux through the mass spectrometer, background and memory effects, influence of the major gaseous component O_2, suitable optical components, their degradation, mass spectral patterns and interference, efficient use of mass peaks at various m/e values to derive trace gas composition, signal processing, information storage, readout, etc. Clearly, a detailed assessment of these aspects is not within the scope of this report. However, even the preliminary ideas and discussion presented in this section indicate the basic feasibility of the application of photoionization mass spectrometry to trace gas analysis of space cabin atmospheres.

REFERENCES

(1) Poschenrieder, W. P. and Warneck, P., "Physics of Planetary Atmospheres IV: Gas Analysis by Photoionization Mass Spectrometry", GCA Technical Report No. 66-1-N January (1966).

(2) Poschenrieder, W. P. and Barrington, A. F., "Development of a Mass Spectrometer Employing a Photoionization Source", GCA Technical Report No. 66-3-N February (1966).

(3) Poschenrieder, W. P. and Warneck P., "Improvement and Optimization of a Mass Spectrometer Employing a Photoionization Source", GCA Technical Report No. 67-12-N June (1967).

(4) Herzog, R. I. and Marmo, F. F., "Mass Spectrometric Determination of Photoionization Products", J. Chem. Phys. 27, 1202 (1957).

(5) Brion, C. E., (a) "A Windowless Photoionization Source for High Resolution Analytical Mass Spectrometers", Anal. Chem. 37, 1706 (1965), (b) "An Improved Mass Spectrometer Photoionization Source", ibid 38, 1941 (1966).

(6) Poschenrieder, W. P. and Warneck, P., "Mass Spectrometric Gas Analysis Utilizing Selective Photoionization", Anal. Chem. 40, 385 (1968).

(7) Kuentzel, L. E., Index of Mass Spectral Data, ASTM Special Publication No. 356, American Society of Testing and Materials, Philadelphia, Pa. (1963).

(8) Gifford, A. P., Rock S. M. and Comaford, D. J., "Mass Spectrometer Analysis of Alcohols and other Oxygenated Derivations" Anal. Chem. 21, 1026 (1949).

(9) Thomas, B. W. and Seyfried, W. D., "Mass Spectrometer Analyses of Oxygenated Compounds", Anal. Chem. 21, 1022 (1949).

(10) Samson, J. A. R., "Techniques of Vacuum Ultraviolet Spectroscopy", J. Wiley, New York (1967) p. 212 ff.

(11) Dibeler, V. H., Walker J. A., and Liston S. K., "Mass Spectrometric Study of Photoionization VII. Nitrogen Dioxide and Nitrous Oxide", J. Res. Nat. Bureau Stand. 71A, 371 (1967).

(12) Watanabe, K., "Photoionization and Total Absorption Cross Sections of Gases. I Ionization Potentials of Several Molecules. Cross Sections of NH_3 and NO", J. Chem. Phys. 22, 1564 (1954).

(13) Schönheit, E., "A Seya-Namioka Monochromator with Toroidal Grating" Optik 23, 305 (1965/66).

NASA-Langley, 1970 — 5 CR-1589